



UNICA

UNIVERSITÀ
DEGLI STUDI
DI CAGLIARI



Università di Cagliari

UNICA IRIS Institutional Research Information System

This is the Author's manuscript version of the following contribution:

Francesco Suriano[#], Claudia Manca[#], Nicolas Flamand, Clara Depommier, Matthias Van Hul, Nathalie M. Delzenne, Cristoforo Silvestri, Patrice D. Cani, Vincenzo Di Marzo.

co-first authors

“Exploring the endocannabinoidome in genetically obese (ob/ob) and diabetic (db/db) mice: links with inflammation and gut microbiota”.

Biochim Biophys Acta Mol Cell Biol Lipids. 2022 Jan;1867(1):159056.

The publisher's version is available at:

[http://dx.doi.org/\[DOI: 10.1016/j.bbalip.2021.159056\]](http://dx.doi.org/[DOI: 10.1016/j.bbalip.2021.159056])

When citing, please refer to the published version.

© <2022>. This manuscript version is made available under the CC-BY-NC-ND 4.0 license <https://creativecommons.org/licenses/by-nc-nd/4.0/>

1 **Exploring the endocannabinoidome in genetically obese (*ob/ob*) and diabetic**
2 **(*db/db*) mice: links with inflammation and gut microbiota.**

3 Francesco Suriano^{1, #}, Claudia Manca^{2,3, #, \$}, Nicolas Flamand², Clara Depommier¹, Matthias Van Hul¹, Nathalie
4 M. Delzenne¹, Cristoforo Silvestri^{2,3}, Patrice D. Cani^{1, *}, Vincenzo Di Marzo^{2,3,4, *}.

5 ¹Metabolism and Nutrition Research group, Louvain Drug Research Institute (LDRI), Walloon Excellence in
6 Life Sciences and BIOTEchnology (WELBIO), UCLouvain, Université catholique de Louvain, Av. E. Mounier,
7 73 B1.73.11, 1200 Brussels, Belgium.

8 ²Quebec Heart and Lung Institute Research Centre, Université Laval, Quebec City, QC G1V 0A6, Canada.

9 ³Centre NUTRISS, Institute of Nutrition and Functional Foods, Université Laval, Quebec City, QC G1V 0A6,
10 Canada.

11 ⁴Endocannabinoid Research Group, Institute of Biomolecular Chemistry, Consiglio Nazionale delle Ricerche,
12 80078 Pozzuoli, Italy.

13 # These authors equally contributed to this work

14 * To whom correspondence should be addressed:

15 Professor Patrice D. Cani, patrice.cani@uclouvain.be (phone number: +32 27647397); Professor Vincenzo Di
16 Marzo, vincenzo.dimarzo@criucpq.ulaval.ca (phone number: 418 656-8711 ext. 7263)

17 \$ current address: Department of Biomedical Science, University of Cagliari, 09042 Monserrato, Italy

18 **Short title:** eCBome and inflammation: learning from *ob/ob* and *db/db* mice

19 **Funding sources:** This work was supported by the Fonds de la Recherche Scientifique (FNRS FRFS-
20 WELBIO) under the grants WELBIO-CR-2017C-02 and WELBIO-CR-2019C-02R, the Funds Baillet-Latour
21 under the grant “Grant For Medical Research 2015”. C.S. and N.F. are associated to the Canada Excellence
22 Research Chair on the microbiome-endocannabinoidome axis in metabolic health, held by V.D. and funded by
23 the Canadian Federal Tri-Agency.

24

25 **Abbreviations**

26 The abbreviations for endocannabinoids and related lipid mediators, receptors and enzymes are listed in
27 Supplemental Table S1 and S2.

28 2-MAGs, 2-acylglycerols; AA, arachidonic acid; Acaca, acetyl-Coenzyme A carboxylase alpha; Adgre1,
29 adhesion G Protein-Coupled Receptor E1; Baat, bile acid-Coenzyme A: amino acid N-acyltransferase;
30 CAconc, cholic acid concentration; CB₁, cannabinoid receptor type 1; CB₂, cannabinoid receptor type 2; Ccl2,
31 chemokine (C-C motif) ligand 2; Cd14, CD14 antigen; Cd163, CD163 antigen; Cd68, CD68 antigen; Cebpa,
32 CCAAT/enhancer binding protein (C/EBP) alpha; CHOLcont, cholesterol content; CLSn, crown-like
33 structures number; Colla1, collagen type I alpha 1; Cpt1a, carnitine palmitoyltransferase 1a liver; Cyp27a1,
34 cytochrome P450 family 27 subfamily a polypeptide 1; Cyp7a1, cytochrome P450 family 7 subfamily a
35 polypeptide 1; Cyp8b1, cytochrome P450 family 8 subfamily b polypeptide 1; eCB, endocannabinoid;
36 eCBome, endocannabinoidome; FM, fat mass; GM, gut microbiota; GPR, G-protein-coupled receptor; Hnf4a,
37 hepatic nuclear factor 4 alpha; Il1b, interleukin 1 beta; Itgax, integrin alpha X; LPS, lipopolysaccharide;
38 LPSconc, lipopolysaccharide concentration; NAEs, N-acylethanolamines; Nlrp3, NLR family pyrin domain
39 containing 3; Oatp1b2, solute carrier organic anion transporter family member 1b2; Ptgs2, prostaglandin-
40 endoperoxide synthase 2; Slc10a1, solute carrier family 10 (sodium/bile acid cotransporter family) member 1;
41 Slc27a5, solute carrier family 27 (fatty acid transporter) member 5; Slc51b, solute carrier family 51 beta
42 subunit; TGcont, triglycerides content; Tgfb1, transforming growth factor beta 1; TLcont, total lipids content;
43 Trl2, toll-like receptor 2; Trl4, toll-like receptor 4; Trl5, toll-like receptor 5; TRPV1, transient receptor
44 potential cation channel subfamily V member 1; WAT, white adipose tissue.

45 **Abstract**

46 **Background:** Obesity and type 2 diabetes are two interrelated metabolic disorders characterized by insulin
47 resistance and a mild chronic inflammatory state. We previously observed that leptin (*ob/ob*) and leptin
48 receptor (*db/db*) knockout mice display a distinct inflammatory tone in the liver and adipose tissue. The present
49 study aimed at investigating whether alterations in these tissues of the molecules belonging to the
50 endocannabinoidome (eCBome), an extension of the endocannabinoid (eCB) signaling system, whose
51 functions are important in the context of metabolic disorders and inflammation, could reflect their different
52 inflammatory phenotypes.

53 **Results:** The basal eCBome lipid and gene expression profiles, measured by targeted lipidomics and qPCR
54 transcriptomics, respectively, in the liver and subcutaneous or visceral adipose tissues, highlighted a
55 differentially altered eCBome tone, which may explain the impaired hepatic function and more pronounced
56 liver inflammation remarked in the *ob/ob* mice, as well as the more pronounced inflammatory state observed
57 in the subcutaneous adipose tissue of *db/db* mice. In particular, the levels of linoleic acid-derived
58 endocannabinoid-like molecules, of one of their 12-lipoxygenase metabolites and of *Trpv2* expression, were
59 always altered in tissues exhibiting the highest inflammation. Correlation studies suggested the possible
60 interactions with some gut microbiota bacterial taxa, whose respective absolute abundances were significantly
61 different between *ob/ob* and the *db/db* mice.

62 **Conclusions:** The present findings emphasize the possibility that bioactive lipids and the respective receptors
63 and enzymes belonging to the eCBome may sustain the tissue-dependent inflammatory state that characterize
64 obesity and diabetes, possibly in relation with gut microbiome alterations.

65 **Keywords:** Endocannabinoids, Liver, Adipose tissue, Lipid signaling, Obesity, Diabetes, Microbiome

66

67 **1. Introduction**

68 During the last years, there has been an upsurge of interest in the expanded endocannabinoid (eCB) system -
69 known as the endocannabinoidome (eCBome) - which comprises several bioactive lipid families biochemically
70 related to the endocannabinoids, their receptors, and metabolic enzymes [1, 2]. The eCBome is widely
71 distributed in various tissues and organs (e.g., brain, liver, intestine, and adipose tissues), and owes its
72 importance to its ability to modulate different physiological functions such as the regulation of glucose and
73 lipid metabolism, food intake, neuroprotection, and inflammation, among others [3-5].

74 The two best characterized endocannabinoids are the arachidonic acid (AA) derivatives, *N*-
75 arachidonylethanolamine, also known as anandamide (AEA), and 2-arachidonoylglycerol (2-AG). They
76 belong respectively to two large distinct families of lipids, the *N*-acylethanolamines (NAEs), and the 2-
77 acylglycerols (2-MAGs). Besides AEA, the NAE family also includes *N*-palmitoylethanolamine (PEA), *N*-
78 stearoylethanolamine (SEA), *N*-oleoylethanolamine (OEA), *N*-linoleylethanolamine (LEA), *N*-
79 eicosapentanoylethanolamine (EPEA), and *N*-docosahexanoylethanolamine (DHEA), while the 2-MAG
80 family encompasses 2-oleoylglycerol (2-OG), and 2-linoleoylglycerol (2-LG), among others. Within their
81 respective families, AEA and 2-AG are the only truly potent and efficacious endogenous agonists of the
82 cannabinoid (CB) receptor type 1 (CB₁) and 2 (CB₂). In addition to the CB receptors, both endocannabinoids
83 can bind and activate the transient receptor potential cation channel subfamily V member 1 (TRPV1). Of note,
84 AEA is a weak agonist of the peroxisome proliferator-activated receptor (PPAR) γ [6, 7]. On the other hand,
85 the other NAEs and 2-MAGs act with varying efficacies at other receptors such as PPAR α or G-protein-
86 coupled receptors 55 (GPR55), 119 (GPR119) and 110 (GPR110) [6]. The levels of endocannabinoids and
87 related mediators are fine-tune regulated by the activity of their synthesizing and degrading enzymes [8].
88 However, studies carried out over the last years have revealed a high degree of redundancy of the metabolic
89 pathways and the corresponding enzymes of these lipids, further highlighting the complexity of the eCBome.
90 Thus, attempting to predict changes in eCBome mediator tissue concentrations based on the observed
91 alterations in the expression of corresponding anabolic and catabolic enzymes is often challenging [9].
92 Furthermore, it is known that the concentrations of the endocannabinoids-like molecules are also regulated by

93 the availability of their ultimate phospholipid precursors and, hence, by the dietary intake of the corresponding
94 fatty acids [10, 11].

95 In the context of metabolic disorders, several studies demonstrated the existence of an association between
96 altered levels or activation of eCB signaling at CB₁ receptors and the development of different pathological
97 conditions such as obesity and type 2 diabetes [11-16], hepatic disorders (i.e., steatosis) [17, 18], and
98 intestinal/adipose tissue inflammation [19, 20]. Conversely, several pieces of evidence suggest that activation
99 of other eCBome receptors, such as CB₂, PPAR α and γ , GPR110, and GPR119 promotes important anti-
100 inflammatory and/or incretin-like effects [21, 22], which can be exploited to improve insulin sensitivity and
101 energy expenditure, thus providing a means for countering obesity-linked metabolic dysfunctions and
102 ameliorating the metabolic status [3, 23]. Other eCBome targets such as TRPV1 and GPR55 instead play both
103 pro-inflammatory and insulin-sensitizing actions [22, 24]. Thus, the functional complexity of the eCBome,
104 and its capacity to differently orchestrate metabolic pathways in different organs and tissues depending on the
105 interplay between ligands and receptors, need further clarification.

106 We have previously shown that genetically obese (*ob/ob*) and diabetic (*db/db*) mice exhibit a distinct gut
107 microbiota (GM) compositions and different Gram-negative bacteria-derived lipopolysaccharide (LPS) levels
108 [25]. We also described that the inflammatory tone of these mice depends on the organ under investigation,
109 with the *ob/ob* model having a more altered hepatic inflammation, while the *db/db* model was characterized
110 by a more inflamed adipose tissue [25]. Our data thus emphasized that the development of obesity and diabetes
111 is specifically organ-dysfunction related. In the present work, we aimed at investigating whether tissue-specific
112 eCBome signaling is associated with the distinct inflammatory phenotypes characterizing *ob/ob* and *db/db*
113 mice. Furthermore, given the existence of a bi-directional relationship between the GM and the eCBome [5,
114 6], we investigated whether the observed differential alterations in the eCBome tone correlate with changes in
115 the composition/function of the GM.

116 **2. Materials and Methods**

117 *2.1 Tissues*

118 The liver and the two adipose tissue depots, i.e., subcutaneous adipose tissue (SAT), and visceral adipose tissue
119 (VAT) used in this study to explore the eCBome tone originated from the same mice used in a previous study
120 and extensively phenotyped in Suriano et al., [25]. All mouse experiments were approved by and performed
121 in accordance with the guideline of the local ethics committee (Ethics committee of the Université catholique
122 de Louvain for Animal Experiments specifically approved this study that received the agreement number
123 2017/UCL/MD/005). Housing conditions were specified by the Belgian Law of 29 May 2013, regarding the
124 protection of laboratory animals (agreement number LA1230314).

125 *2.2 Lipid extraction and HPLC-MS/MS for the analysis of eCBome mediators*

126 Lipids were extracted from tissue samples according to the Bligh and Dyer method [26]. Briefly, about 10mg
127 of liver and adipose tissues were sampled and homogenized in 1ml of a 1:1 Tris-HCl 50mM pH 7: methanol
128 solution containing 0.1M acetic acid and 5ng of deuterated standards. One ml of chloroform was then added
129 to each sample, which were then vortexed for 30 seconds and centrifuged at 3000×g for 5 minutes. The organic
130 phase was collected and another 1 ml of chloroform was added to the inorganic one. This was repeated twice
131 to ensure the maximum collection of the organic phase. The organic phases were pooled and evaporated under
132 a stream of nitrogen and then suspended in 50µl of mobile phase containing 50% of solvent A (water + 1mM
133 ammonium acetate + 0,05% acetic acid) and 50% of solvent B (acetonitrile/water 95/5 + 1mM ammonium
134 acetate + 0.05% acetic acid). Forty µl of each sample were finally injected onto an HPLC column (Kinetex C8,
135 150 × 2.1mm, 2.6µm, Phenomenex) and eluted at a flow rate of 400µl/min using a discontinuous gradient of
136 solvent A and solvent B [27]. Quantification of eCBome-related mediators (supplemental Table S1), was
137 carried out by HPLC interfaced with the electrospray source of a Shimadzu 8050 triple quadrupole mass
138 spectrometer and using multiple reaction monitoring in positive ion mode for the compounds and their
139 deuterated homologs.

140 In the case of unsaturated monoacylglycerols, the data are presented as 2-monoacylglycerols (2-MAGs) but
141 represent the combined signals from the 2- and 1(3)-isomers since the latter are most likely generated from the
142 former via acyl migration from the *sn*-2 to the *sn*-1 or *sn*-3 position.

143 *2.3 RNA isolation, Reverse Transcription and qPCR-based TaqMan Open Array*

144 Total RNA was prepared from collected tissues using TriPure reagent (Roche). Quantification and integrity
145 analysis of total RNA was performed by running 1µl of each sample on an Agilent 2100 Bioanalyzer (Agilent
146 RNA 6000 Nano Kit, Agilent, Santa Clara, CA, USA). All samples had a RNA integrity number (RIN) above
147 6. cDNA was prepared by reverse transcription of 1µg total RNA using a Reverse Transcription System Kit
148 (Promega, Madison, Wisconsin, USA).

149 Sixty-five nanograms of starting RNA were used to evaluate the expression of the 52 eCBome-related genes
150 and 4 housekeeping genes (supplemental Table S2) using a custom-designed qPCR-based TaqMan Open Array
151 on a QuantStudio 12K Flex Real-Time PCR System (Thermo Fisher Scientific, CA, USA) following the
152 manufacturer's instructions. Samples were analyzed randomly. mRNA expression levels were calculated from
153 duplicate reactions using the $2^{-\Delta\Delta C_t}$ method as calculated by CFX Maestro Software (Bio-Rad) and are
154 represented as fold change with respect to baseline within each tissue. *Rps 13* was used as reference gene.

155 *2.4 Correlation analysis*

156 As previously described [28], correlation analysis between two data sets of variables were performed using the
157 R package 'psych' (version 2.1.6). Based on the normality of the data distribution, a parametric test (i.e.,
158 Pearson) which assumes a normal distribution, or a non-parametric test (Spearman) which assumes a non-
159 normal distribution of the data were used. In detail, Pearson's rank test and the Bonferroni's adjustment were
160 used when correlating metabolic parameters with the eCBome, whereas Spearman's rank test and Holm's
161 adjustment were used when correlating the bacterial taxa with the eCBome. All statistical analyses were
162 performed on RStudio (version 4.1.0, Rstudio Team, Boston, MA, USA).

163 *2.5 Statistical analysis*

164 Data are presented as the mean±standard error of the mean (S.E.M), as specified in the individual tables and
165 figures. The differences between the groups were determined using a One-Way ANOVA followed by Tukey's
166 post hoc test on $\Delta\Delta\text{Ct}$ and on fmol/mg tissue for gene expression levels and mediator levels respectively.
167 Only statistically significant differences between *ob/ob* and *db/db* mice were reported. The differences between
168 experimental groups were considered statistically significant with $P\leq 0.05$ and represented as follows: * P
169 ≤ 0.05 , ** $P \leq 0.01$, *** $P \leq 0.005$, **** $P \leq 0.001$. Data were analyzed using GraphPad Prism version 8.00 for
170 Windows (GraphPad Software). The presence of outliers was assessed using the Grubbs test.

171 **3. Results**

172 *3.1 Different eCBome profiles in the liver of ob/ob and db/db mice*

173 We previously showed that *ob/ob* mice are characterized by a more pronounced inflammatory response in the
174 liver as compared to *db/db* mice[25]. Looking for potential mechanisms and causal factors, we found that the
175 two mutant models display distinct hepatic bile acids profiles and gut microbiota composition [25]. Since there
176 is a cross-talk between the gut microbiota and bioactive lipids belonging to the eCBome, which have been
177 implicated in several physiological and pathological conditions [5, 13, 29], we wondered whether the different
178 inflammatory tones were also associated with differential eCBome profiles. Accordingly, we measured the
179 concentration of a panel of eCBome-related mediators in tissues from the mice used in the previous study [25],
180 and performed transcriptomic analysis looking at the gene expression of their corresponding anabolic and
181 catabolic enzymes, as well as their receptors (Figure 1A, B and supplemental Table S3). Although several
182 alterations in both genetic models were found, we discuss hereafter only those that were significantly different
183 between *ob/ob* and *db/db* mice and hence might underlie the observed differences in inflammation-related
184 indicators. Other alterations noted in the hepatic tissue are shown in supplemental Table S3. Concerning the
185 eCBs and related molecules (Figure 1A), we did not find any significant change in the hepatic concentrations
186 of the two endogenous ligands of CB₁ and CB₂ receptors, 2-AG and AEA (data not shown). Conversely, we
187 observed a statistically significant decrease of the 2-acylglycerol derivative (i.e., 2-LG) and the ethanolamine
188 derivative (i.e., LEA) of linoleic acid (LA), in *ob/ob* mice with respect to *db/db* mice. 13-HODE-G, which is
189 a novel molecule derived from the 12-lipoxygenase-catalysed oxygenation of 2-LG [30], displayed also
190 significantly lower levels in *ob/ob* compared to *db/db* mice. The levels of the omega-3 fatty acid,
191 eicosapentaenoic acid (EPA), and its derivative 2-EPG were also decreased in *ob/ob* mice with respect to the
192 diabetic group, although the latter difference did not reach statistical significance ($P = 0.072$). Accordingly,
193 the levels of 15- and 18-HEPE, which are both EPA bioactive metabolites, were also significantly reduced in
194 the *ob/ob* compared to *db/db* group. The 2-DPG, which derives from another omega-3 fatty acid, DPA,
195 presented also a trend towards lower levels in *ob/ob* mice compared to *db/db* mice, whilst the amounts of the
196 derivative of the omega-3 fatty acid DHA, 2-DHG, displayed an opposite and strongly significant increase in
197 *ob/ob* with respect to *db/db* mice. However, no significant differences were observed in the concentration of

198 DPA and DHA between the two groups (data not shown). The hepatic levels of two main NAEs, OEA and
199 PEA, were also significantly higher in *ob/ob* than *db/db* mice as were those of the 2-monoacylglycerol 2-OG.
200 We also examined the hepatic concentration of non-eCBome mediators such as the prostaglandins, and found
201 a significant increase of PGD₂ and PGE₂ levels in *ob/ob* with respect to *db/db* mice.

202 We then investigated if the changes found in the levels of the eCBome mediators were accompanied by
203 modulation of the mRNA expression of their anabolic and catabolic enzymes or receptors (Figure 1B).
204 Regarding receptors, there were statistically significant changes in the expression of *Pparg*, *Ptgfr* and *Trpv2*,
205 which were augmented in the liver of *ob/ob* with respect to the *db/db* mice. Stronger differences in gene
206 expression were observed at the level of eCBome-related metabolic enzymes. Specifically, there was a global
207 significant increase, in *ob/ob* compared to *db/db* mice, of: 1) the transcript levels of NAE biosynthetic
208 enzymes, i.e. *Abhd4*, *Gdpd1*, *Inpp5d* and *Napepld*, which could potentially explain the increase of hepatic
209 PEA and OEA levels in the *ob/ob* group, and 2) the transcript levels of MAG catabolic enzymes *Ces1d* and
210 *Mgll*, which might instead explain the lower levels of 2-LG and 2-EPG, but not 2-DHG, in these mice.

211 Altogether, these results highlight a different anti-inflammatory hepatic eCBome profile between *ob/ob* and
212 *db/db* mice, which may partially explain the earlier onset of liver inflammation and impaired liver function
213 observed in *ob/ob* mice as found in Suriano et al., [25].

214 3.2 Different eCBome profiles in the adipose tissues of *ob/ob* and *db/db* mice

215 Despite the lower inflammatory tone in the liver, *db/db* mice displayed elevated inflammation-related
216 parameters in both subcutaneous and visceral adipose tissue (SAT and VAT) depots, with the SAT presenting
217 the most pronounced inflammatory phenotype [25].

218 In this latter tissue (Figure 2A), we found no difference for the endocannabinoid 2-AG between the *ob/ob* and
219 *db/db* mice (data not shown). However, the 2-acylglycerols 2-PG, 2-OG and 2-DHG, and the 2-LG 12-
220 lipoygenase metabolite, 13-HODE-G were all decreased in *db/db* with respect to *ob/ob* mice, while 2-LG
221 presented only a trend towards a decrease. Regarding NAEs, there were no differences, whereas significantly
222 higher levels of the omega-3 fatty acids EPA and DPA were present in the *db/db* compared to the *ob/ob* group.
223 In the VAT (Figure 3A), despite clear trends, no statistically significant differences were observed for almost

224 all the molecules studied, the only exceptions being AEA and *N*-docosahexaenylethanolamine (DHEA), the
225 levels of which were significantly decreased in the *db/db* group.

226 Concerning the genes encoding eCBome-related receptors (Figure 2B and 3B), for SAT and VAT,
227 respectively), *Cnr2*, *Pparg* and *Trpv2* were the only ones showing differential gene expression between the
228 *ob/ob* and *db/db* groups. In particular, while in SAT the transcript levels of these receptors were significantly
229 modified, with *Cnr2* and *Trpv2* showing an increased expression in *db/db* respect to *ob/ob* mice and *Pparg*
230 having an opposite significant trend, in VAT the changes were in the same direction as SAT but statistically
231 significant only for *Pparg* and *Trpv2*.

232 Regarding eCBome anabolic and catabolic enzymes, significant differences were found for the gene expression
233 of 2-monoacylglycerol biosynthetic enzyme *Plcb1*, the lipoxygenase *Alox12* and the NAE anabolic enzyme
234 *Gde1*. Specifically, whilst in SAT only the mRNA expression of *Plcb1* and *Alox12* displayed a significant
235 decrease in the *db/db* group, in the VAT there was a statistically significant reduction also for *Gde1*. The
236 decreased transcript levels of *Plcb1* in the SAT could explain the observed reduction of most 2-acylglycerols,
237 although the decreased expression was stronger in the VAT, where we found no significant decrease in these
238 mediators. Also, the decrease in the expression of SAT *Alox12* and of VAT *Gde1* in the *db/db* mice, might
239 explain the reduction, in the *db/db* group, of SAT 13-HODE-G and of VAT NAEs levels, respectively. Other
240 alterations remarked in both adipose tissue depots are shown in supplemental Table S4 and Table S5, for SAT
241 and VAT, respectively.

242 The aforementioned results highlight an anti-inflammatory mediator profile that was more markedly modified
243 in the SAT than in the VAT when comparing *ob/ob* and *db/db* mice, thus possibly explaining in part the more
244 pronounced inflammatory phenotype in this tissue. Conversely, receptor and enzyme expression were similarly
245 modified in the two adipose depots. Globally, these results seem to fit with the increase of the inflammation-
246 related parameters in *db/db* with respect to *ob/ob* mice as observed in Suriano et al., [25].

247 *3.3 Correlations between eCBome mediators and inflammation in the liver and the two adipose tissue* 248 *depots*

249 Given the different eCBome profiles observed in the liver and the two adipose tissue depots between *ob/ob*
250 and the *db/db* mice, we explored correlations between previously obtained metabolic parameters in these three

251 different biological sites and published in Suriano et al., [25], and eCBome mediator tissue concentrations or
252 metabolic enzyme and receptor mRNA expression levels. Analysis of the Pearson's rank correlation matrix
253 confirmed the existence of potential links between certain eCBome-lipids and genes and several metabolic
254 parameters. In details, starting from the liver, the matrix correlation showed that LA, 2-LG, and LEA were
255 negatively correlated with liver weight, markers associated with a steatosis state (i.e., total lipid (TL) content,
256 triglyceride (TG) and cholesterol (CHOL) content), immune cell recruitment markers (i.e., *Itgax*, crown-like
257 structures number (CLS_n)), and a marker associated with a fibrosis state (*Tgfb1*), and a bile acid metabolism
258 marker (i.e., *Abcb4*); EPA was positively correlated with a bile acid metabolism marker (*Slc27a5*); 15-HEPE
259 was positively correlated with the LPS concentration; 2-DHG, and 2-OG were positively correlated with
260 markers of steatosis (i.e., TL content), immune cell recruitment and inflammatory markers (i.e. *Ccl2*, *Itgax*,
261 CLS_n, *Cd14*, *Tlr2*), fibrosis markers (i.e., *Colla1*, *Tgfb1*), and bile acid metabolism marker (i.e., *Slc51b*); PGE₂
262 was positively associated with immune cells recruitment markers (i.e., *Ccl2*, *Cd68*). In addition, most of the
263 receptors and metabolic enzymes for the eCBome-mediators were positively correlated with the final body
264 weight, final fat mass (FM), liver weight, steatosis (i.e., TL, TG and CHOL content), immune cell recruitment
265 and inflammation markers (i.e., *Ccl2*, *Itgax*, *Cd68*, CLS_n, *Cd14*, *Tlr4*, *Tlr2*, *Tlr5*, *Nlrp3*, *Tnf*, *Il1b*), fibrosis
266 markers (i.e., *Colla1*, *Tgfb1*), and bile acid metabolism markers (*Abcb4*, *Slc51b*); and negatively correlated
267 with other bile acid metabolism markers (*Cyp27a1*, *Slc10a1*, *Oatp1b2*) (Figure 4).

268 Contrary to what we observed in the liver, we found that, in the SAT, 2-PG, 2-OG, 2-LG, and *Plcb1* were
269 positively correlated with the inflammatory marker *Tlr5*; DPA was positively correlated with SAT weight,
270 LPS concentration, and a marker of immune cell recruitment (i.e., *Ccl2*); similarly, *Cnr2* was positively
271 correlated with another marker of immune cell recruitment (i.e., *Cd68*) (Figure 5A). On the other hand, in the
272 VAT, *Cnr2* was positively correlated with final body weight, final FM, VAT weight, LPS concentration,
273 immune cell recruitment and inflammatory markers (i.e., *Ccl2*, *Adgre1*, *Itgax*, *Cd68*, *Tlr4*, *Tlr2*, and *Il1b*);
274 *Pparg* and *Gde1* were both negatively correlated with final body weight, final FM, VAT weight, LPS
275 concentration, immune cell recruitment, and inflammation markers (i.e., *Adgre1*, *Itgax*, *Cd68*, and *Il1b*)
276 (Figure 5B). Taken together, these observations highlight how eCBome signaling may be involved in
277 modulating, or being modulated by, various metabolic and inflammatory pathways in three different biological
278 sites, whose functions are closely related to obesity and associated metabolic disorders.

279 3.4 Correlations between eCBome mediators and gut microbiota taxa with emphasis on taxa involved
280 in inflammation

281 Changes in the composition of the GM could partly underlie, or be caused by, alterations in eCBome signaling
282 described above, thereby contributing both directly and indirectly to the different inflammatory tone described
283 in the liver and the two adipose tissue depots. To this end, we investigated the existence of correlations between
284 eCBome mediator tissue concentrations or metabolic enzyme and receptor mRNA expression levels and the
285 relative abundance of bacterial taxa that were significantly, or tended to be, different between *ob/ob* and *db/db*
286 mice. When exploring such correlations using Spearman's rank correlation matrix, we observed that several
287 bacterial taxa belonging to the *Firmicutes* phylum were either positively or negatively correlated with the
288 eCBome signaling. In details, *Clostridium_sensu_stricto_1*, was negatively correlated with hepatic
289 concentrations of 2-LG, 13-HODE-G, and EPA, and positively correlated with PEA and PGD₂; *Dubosiella*,
290 was positively correlated with PGD₂; *Lachnospiraceae_UCG_006*, was positively correlated with 15-HEPE;
291 *Turicibacter*, was negatively correlated with EPA and positively correlated with PEA, PGE₂, and PGD₂. On
292 the other hand, *Rikenellaceae_RC9_gut.group*, belonging to the *Bacteroidetes* phylum was negatively
293 correlated with PEA and PGD₂; *Bacteroides*, belonging to the same phylum was negatively correlated with
294 PGD₂ (Figure 6). We also found that *Clostridium_sensu_stricto_1* was positively correlated with the SAT 13-
295 HODE-G and *Pparg*, while *Turicibacter* was positively correlated with the SAT 2-DHG and 13-HODE-G
296 (Figure 7A). The same bacterial taxa, as well as *Dubosiella*, were both positively correlated with the VAT
297 level of *Plcb1* (Figure 7B). These correlative data suggest the existence of a direct or indirect cross-talk
298 between eCBome signaling in the liver, SAT or VAT and the GM.

299

300 4. Discussion

301 In the present study, we aimed at exploring whether alterations, either at the transcription level or in terms of
302 tissue concentrations of molecules belonging to the eCBome, a complex signaling system whose dysregulation
303 is associated with different pathological conditions (e.g., obesity, type 2 diabetes) [1, 13, 18, 31], could reflect
304 the different inflammatory phenotypes that we previously observed in genetically obese (*ob/ob*) and diabetic
305 (*db/db*) mice [25]. Although both mutant mice exhibit the same body weight and fat mass gain evolution over
306 the course of the experiment, they develop distinctive inflammatory phenotypes, with the liver being more
307 inflamed in *ob/ob* mice, and the adipose tissues being more inflamed in *db/db* mice. Despite a different
308 underlying molecular mechanism at the basis of leptin signaling deficiency in *ob/ob* and *db/db* mice (ligand
309 versus receptor, respectively) [32], many mechanistic details associating impaired leptin signaling with the
310 development of inflammation in *ob/ob* and *db/db* mice remain poorly investigated and need further
311 investigation. Likewise, the relevance of findings obtained in these mice to diet-induced obesity and ensuing
312 systemic and organ inflammation also remains to be fully explored. Seeking for a causal factor, the results we
313 provide are unique since they represent a comprehensive investigation of how bioactive lipids as well as
314 receptors and enzymes belonging to eCBome and related prostaglandin signaling may potentially sustain or
315 counteract the tissue-dependent inflammatory state in mice having the same body weight but different glucose
316 homeostasis. We identified the presence of a possible inflammation-related molecular profile, since some of
317 the observed alterations were characteristic of all tissues showing the most pronounced inflammatory response,
318 i.e.: 1) 2-LG and its 12-lipoxygenase metabolite 13-HODE-G [30] were present in reduced concentrations, and
319 2) *Trpv2* showed increased expression, in both the liver of *ob/ob* mice and the adipose tissue depots of *db/db*
320 mice. While still little is known about the receptors of 13-HODE-G, the levels of the established targets for 2-
321 LG, i.e. GPR119 and TRPV1 (activated by all saturated and polyunsaturated 2-MAGs [33]), were not modified
322 in either liver and adipose tissues of obese and diabetic mice. Interestingly, GPR119 is also activated by: 1) 2-
323 OG, whose levels were also reduced in the liver and SAT of *db/db* mice, and 2) LEA, a NAE whose levels
324 were significantly decreased in the liver of *ob/ob* mice. Regarding the non-selective cation channel *Trpv2*, its
325 expression in immune cells suggests a role in the immune response and inflammation [34, 35], and, in
326 hepatomas, a stimulatory function on oxidative stress [36]. To date, the only eCBome mediators that have been

327 shown to act as TRPV2 ligands are the unsaturated long chain NAEs, such as LEA, which were found to
328 antagonize this channel [37]. Therefore, we hypothesize that the more pronounced inflammatory tone in the
329 liver and adipose tissues of *ob/ob* and *db/db* mice, respectively, might be due in part to higher expression of
330 *Trpv2* and, in the former case, to the lower levels of its endogenous antagonist LEA. However, the contribution
331 of TRPV2 to inflammation requires further investigations, and *in vitro* and *in vivo* experiments are needed to
332 elucidate its role in the context of obesity.

333 In addition to those mentioned above, other tissue-specific inflammation-related changes were observed. We
334 found significantly decreased levels of the omega-3 fatty acid EPA and its derivatives in *ob/ob* mice,
335 characterized by inflammation-related hepatic injuries. It is known that n-3 PUFAs exert metabolic benefits,
336 which may also result from the elevation of their corresponding NAEs and 2-MAGs [38], as well as other *N*-
337 acylamides [39], which possess anti-inflammatory and anti-cancer actions and potential cardiometabolic and
338 neuroprotective effects independent of cannabinoid receptors [40-43]. In agreement with this hypothesis, and
339 with the reduced availability of EPA, we also remarked a decrease of the eCBome EPA derivative, 2-EPG, as
340 well as of the bioactive metabolites 15- and 18-HEPE, in the liver of *ob/ob* mice. In contrast, we found
341 increased levels of the DHA-derived 2-DHG in *ob/ob* mice, possibly as a compensatory mechanism to
342 counteract the stronger hepatic inflammation observed in this group. Indeed, a recent study in humans with
343 abdominal obesity and low-grade systemic inflammation showed that DHA may produce stronger anti-
344 inflammatory effects as compared to EPA [44]. The increased hepatic levels of DHA derivative (i.e. 2-DHG)
345 vs. EPA may be due to a more efficacious conversion of EPA into DHA in *ob/ob* mice as compared to their
346 controls, a possibility that deserves further investigation. On the other hand, the increased levels of the two
347 omega-3 PUFAs, EPA and DPA, in the more inflamed SAT of *db/db* mice led us to speculate about a possible
348 negative feedback mechanism; however, the statistically significant reduced levels of the 2-DHG in this tissue
349 were in agreement with a more pronounced inflammatory status. Regarding the VAT, we only observed
350 reduced levels of the DHA-derived NAE, DHEA, which is known to exert anti-inflammatory effects in several
351 inflammation models [41] as well as in LPS-induced inflammation in adipocytes [45], and might, therefore
352 partly explain the higher inflammatory tone in the VAT of *db/db* mice. Accordingly, the expression levels of
353 the nuclear receptor *Pparg*, which has been suggested to partially mediate, together with CB₂, DHEA anti-
354 inflammatory actions [45], were significantly decreased in the VAT of *db/db* mice.

355 Previous *in vitro* and *in vivo* studies have also described altered NAE and 2-MAG levels, together with an
356 excessive activation/expression of CB₁, in the liver and adipose tissue both at the cellular and tissue levels
357 during obesity and diabetes, thereby leading to altered lipid and glucose metabolism as well as inflammation
358 [3, 15, 46]. Consistently, *Cnr1* (encoding CB₁)-KO mice are protected against diet-induced obesity [15].
359 However, in our study, no change in the expression of *Cnr1* was observed, nor in the levels of the
360 endocannabinoid 2-AG in all the tissues considered, or of AEA hepatic and SAT levels, thus suggesting that
361 CB₁ activation by AEA or 2-AG is not the main contributor to the stronger hepatic and adipose tissues
362 inflammation observed in *ob/ob* and *db/db* mice, respectively. In the VAT, in fact, the levels of AEA were
363 significantly reduced in *db/db* compared to *ob/ob* mice, possibly in agreement with the decreased expression
364 levels of the *Pparg*, which has been shown to be transcriptional activated by AEA in the micromolar
365 concentration range [47, 48], to stimulate the differentiation of fibroblasts to adipocytes [47], and to exert anti-
366 inflammatory effects [49].

367 Despite a more-pronounced liver inflammation, we observed increased hepatic levels of the two AEA
368 congeners, OEA and PEA in *ob/ob* mice. Previous *in vitro* and *in vivo* studies have already described the anti-
369 inflammatory, analgesic and neuroprotective effects exerted by OEA and PEA through PPAR α -dependent
370 mechanisms [50-52]. Furthermore, administration of PEA induced significant improvement in a rat model of
371 liver fibrosis, possibly by inhibiting the activation of hepatic stellate and Kupffer cells [53]. It is therefore
372 possible that increased hepatic levels of OEA and PEA in *ob/ob* mice, together with higher hepatic expression
373 of *Pparg*, are the result of compensatory mechanisms aimed at counteracting the hepatic inflammation and
374 fibrosis observed in this model. A similar compensatory mechanism may have occurred in the SAT (and, in a
375 non-statistically significant manner, in the VAT) of *db/db* mice through an increased expression of the eCB
376 receptor, *Cnr2*, a well-characterized anti-inflammatory receptor, known to be upregulated in a plethora of
377 inflammatory conditions [54, 55].

378 From a more mechanistic point of view, the observed increase in the hepatic levels of some NAEs may be due
379 to the increased expression of *Napepld*, the main anabolic enzymes for NAEs, as well as of other anabolic
380 enzymes (i.e., *Abhd4*, *Gdpd1*, *Inpp5d*), which may also partially contribute to NAE biosynthesis [56]. We
381 recently discovered that NAPE-PLD is a key regulatory enzyme whose function may go beyond the synthesis
382 of NAEs, since its hepatocyte-specific deletion in mice was associated also with a marked modification of

383 various bioactive lipids involved in host homeostasis, such as the bile acids (BAs) [57]. On the other hand,
384 Margheritis et al., [58] demonstrated that BAs (i.e., deoxycholic acid) in turn modulate NAPE-PLD activity.
385 We can therefore not exclude that the increased expression of *Napepld* may also be due to cholic acid, a primary
386 bile acid, whose hepatic concentration is increased in *ob/ob* mice [25]. To date, however, there are no studies
387 describing the modulation of NAPE-PLD by cholic acid and further investigations are needed in this direction.
388 That being said, increased hepatic *Napepld* expression may explain the higher OEA and PEA levels, but not
389 the lower LEA concentrations, in the liver, thus indicating that NAE biosynthesis is regulated by different
390 enzymes as well as by precursor availability (which, in the case of LEA, was indeed reduced in *ob/ob* mice).
391 Likewise, the higher hepatic expression levels of 2-MAG-hydrolysing enzymes, i.e. carboxylesterase 1D
392 (*Ces1d*) and, particularly, *Mgll*, might explain the lower levels of 2-LG, but not the increase of 2-OG, in *ob/ob*
393 mice. Instead, in the SAT, the generalized decrease in 2-MAGs (but not 2-AG) observed in *db/db* mice may
394 have resulted from the decreased expression of *Plcb1*, encoding the enzyme catalyzing the rate-limiting
395 reaction in 2-MAG biosynthesis. However, *Plcb1* was also down-regulated in the VAT, where 2-MAG levels
396 were not different between *ob/ob* and *db/db* mice. Finally, reduced expression of the NAE-biosynthetic
397 enzyme, *Gde1*, was observed only in the VAT and so were the reduced concentrations of AEA and DHEA,
398 but not of other NAEs, whereas the observed decrease in the expression of *Alox12* may explain the reduction
399 in the levels of 13-HODE-G in the SAT, but not the lack of changes in this metabolite found in the VAT.

400 An additional potential mechanism underlying metabolic disorder-associated inflammation may be represented
401 by the increase of two pro-inflammatory eicosanoids, the prostaglandins PGE₂ and PGD₂ as well as of the
402 expression of the prostaglandin F_{2α} receptor *Ptgfr* observed in the liver of *ob/ob* mice compared to *db/db* mice
403 [59].

404 Looking for specific links between eCBome-signaling and the metabolic parameters measured in the three
405 different biological sites, we carried out correlation analyses and observed that eCBome mediator or metabolic
406 enzyme/receptor gene expression levels were either positively or negatively correlated with several metabolic
407 parameters linked to steatosis, recruitment of immune cells, and inflammation. This suggests that this complex
408 endogenous signaling system may affect the metabolic function of the respective tissues. In particular, we
409 noticed that hepatic 15-HEPE, suggested to act as an anti-inflammatory bio-active lipid [60, 61], was positively

410 correlated with LPS levels, which may reflect a negative feedback response of the *db/db* mice aimed at
411 counteracting steatosis, inflammation, and fibrosis. Increased circulating levels of LPS, a condition known as
412 metabolic endotoxemia, were previously associated with obesity, insulin resistance, hepatic lipid
413 accumulation, liver and adipose tissue inflammation [62-64]. The levels of the TRPV2 antagonist, LEA, and
414 of 2-LG, were negatively correlated with hepatic TG content, which in turn is directly related to hepatic
415 inflammation, thus supporting the aforementioned potent protective role of these two eCBome mediators
416 against liver inflammation in *ob/ob* mice. Additionally, on the one hand, PGE₂ levels, *Ptgfr*, *Mgll*, and *Trpv2*
417 gene expression, and, on the other hand, *Pparg*, *Napepld*, and *Gde1* gene expression, which, as discussed
418 above, have been associated with inflammation and immune cell recruitment or protection against it,
419 respectively, were positively correlated with immune and inflammatory markers, liver weight or TG content,
420 thus strengthening their possible role in causing, or attempting to adapt to, the higher lipid accumulation and
421 inflammatory tone in the liver of *ob/ob* mice. In the two adipose tissues, fewer correlations were observed
422 between eCBome signaling and metabolic parameters, which could suggest that other factors, in addition to
423 the altered eCBome, may be implicated in the modulation of the inflammatory tone observed in the SAT and
424 VAT, particularly in *db/db* mice. Nevertheless, we did observe the expected positive correlation between *Cnr2*
425 and the macrophage marker *Cd68* in the SAT as well as with other inflammatory markers in the VAT, and
426 negative correlations between *Pparg* and *Gde1* and LPS and other inflammatory markers in this adipose tissue
427 depot, thus substantiating some of the speculations made above regarding the role of these eCBome members
428 in adipose tissue inflammation in *db/db* mice. *Pparg* was also negatively correlated with VAT weight, but this
429 may reflect the positive correlation between the latter and LPS, which inhibits adipocyte differentiation, with
430 subsequent adipocyte death, recruitment of immune cells and inflammation, which are all typical features of
431 *db/db* mice [46, 65].

432 Among the factors contributing to both hepatic and adipose tissue inflammation in obesity, we have previously
433 shown that the gut microbiota may act as a key modulator, notably through the LPS-eCB system regulatory
434 loops, of the adipose tissue metabolism/function and general lipid homeostasis regulation in the liver [46]. The
435 gut microbiota has indeed been proposed to regulate levels of endocannabinoids in the adipose tissue and the
436 gut, and changes in its composition are sufficient to reduce peripheral eCB system tone in genetically induced
437 and diet-induced models of obesity [5]. To provide indirect evidence that the gut microbiota plays a role in

438 determining eCBome participation in the inflammatory phenotype of *ob/ob* mouse livers or *db/db* mouse
439 adipose tissue, we analyzed the correlation between the eCBome members and the absolute abundance of
440 certain fecal bacterial taxa that were different between the two mutant mice models [25]. Interestingly, some
441 bacterial taxa were either positively or negatively correlated with certain eCBome-related molecules and
442 receptors. Among them, *Clostridium_sensu_stricto_1* deserves particular attention since its absolute quantity
443 was significantly higher in *ob/ob* mice than in *db/db* mice and was positively correlated with either pro-
444 inflammatory (i.e., PGD2) or anti-inflammatory (i.e., PEA) hepatic bioactive lipids, and negatively correlated
445 with other anti-inflammatory bioactive lipids (i.e., 2-LG, 13-HODE-G, and EPA). As a matter of fact, recent
446 findings in humans and mice showed that this bacterial taxon was positively correlated with indicators of body
447 weight and serum lipids [66], and with all non-alcoholic fatty-liver disease parameters [67]. In our present
448 study, the same bacterial taxon was positively correlated with the levels of the putative anti-inflammatory lipid
449 13-HODE-G, and *Pparg* expression, measured in the SAT, suggesting a negative feedback response aiming at
450 counteracting inflammation, whereas in the VAT *Clostridium_sensu_stricto_1* was positively correlated with
451 *Plcb1* expression.

452 Taken together, the results from our correlational analyses reinforce the hypothesis that the different profiles
453 of eCBome signaling observed in the liver and adipose tissue depots of *ob/ob* and *db/db* mice may contribute
454 to the respective inflammatory phenotypes in these tissues. However, more studies are needed to elucidate
455 whether the identified eCBome-related molecules and their respective receptors and enzymes have a causal
456 role in inflammation in these two genetically obese mice models. Indeed, the major limitation of this study
457 consists in the lack of new *in vitro* experiments to elucidate the mechanisms of action of the eCBome members
458 found to undergo differential changes in this study, and the reliance on previously published data on this aspect.
459 Consequently, our correlation analyses do not imply causation and will require further studies.

460 In conclusion, the present study shows potential divergences in eCBome signaling between *ob/ob* and *db/db*
461 mice that could be related to the etiology or consequences of the different inflammatory tone observed in the
462 liver and the adipose tissue depot of these two mutant strains. The identification of such bioactive lipids and
463 their related receptors and anabolic/catabolic enzymes may represent the basis of novel therapeutic approaches
464 to tackle inflammation, which is a well-known common feature associated with obesity and diabetes. Besides,

465 this work identified host-microbiome-eCBome interactions whose relevance in the context of obesity-related
466 inflammation needs to be further assessed by means of mechanistic studies.

467 **Data Availability**

468 Data are showed within the manuscript and in the supplemental information files. For the correlation analysis
469 between the eCBome signaling and the gut microbiota, we re-used the microbial data previously published in
470 Suriano et al., [25]. The raw amplicon sequencing data are available in the European Nucleotide Archive
471 (ENA) at EMBL-EBI under accession number PRJEB44809.

472 **Declaration of interest**

473 None.

474 **Authors' Contributions:**

475 Conceptualization: F.S., P.D.C. and V.D. Methodology: F.S., C.M., N.F., P.D.C., V.D. Correlation analysis:
476 F.S. and C.D. Funding acquisition: P.D.C., V.D., C.S., N.F. Investigation: F.S., C.M., N.F., C.D., M.V.H., C.S.
477 Supervision: P.D.C and V.D. Resources: P.D.C., N.M.D., C.S., N.F., V.D. Writing - Original Draft: F.S., C.M.,
478 P.D.C. and V.D. Writing - Review & Editing: all the authors. All authors have read and agreed to the published
479 version of the manuscript.

480 **Acknowledgments**

481 We thank B. Es Saadi, A. Puel and C. Martin for their excellent technical assistance. We thank M. Verce for
482 help with data visualization using R Studio. P.D.C. is a senior research associate at FRS-FNRS (Fonds de la
483 Recherche Scientifique), Belgium. C.M. was the recipient of a post-doctoral boursary from the Joint
484 International Research Unit on Chemical and Biomolecular Studies on the Microbiome and its Impact on
485 Metabolic Health and Nutrition (JIRU-MicroMeNu), which is funded by the Sentinelle Nord-Apogée Program
486 of Université Laval, funded in turn by the Federal Tri-Agency of Canada. V.D. is the holder of the Canada
487 Excellence Research Chair on the Gut Microbiome-Endocannabinoidome Axis in Metabolic Health (CERC-
488 MEND) at Université Laval, funded by the Federal Tri-Agency of Canada. V.D. is the recipient of two Canada
489 Foundation for Innovation grants (37392 and 37858).

490

491 **References**

- 492 [1] L. Cristino, T. Bisogno, V. Di Marzo. (2020). Cannabinoids and the expanded endocannabinoid system in
493 neurological disorders. *Nat Rev Neurol*, 16(1), 9-29. doi:10.1038/s41582-019-0284-z
- 494 [2] V. Di Marzo, and Wang, J. ((eds) (2015)). *The Endocannabinoidome: The World of Endocannabinoids and*
495 *Related Mediators*. USA:Academic Press Books-Elsevier.
- 496 [3] A. Veilleux, V. Di Marzo, C. Silvestri. (2019). The Expanded Endocannabinoid
497 System/Endocannabinoidome as a Potential Target for Treating Diabetes Mellitus. *Curr Diab Rep*, 19(11),
498 117. doi:10.1007/s11892-019-1248-9
- 499 [4] V. Di Marzo. (2020). The endocannabinoidome as a substrate for noneuphoric phytocannabinoid action
500 and gut microbiome dysfunction in neuropsychiatric disorders. *Dialogues Clin Neurosci*, 22(3), 259-269.
501 doi:10.31887/DCNS.2020.22.3/vdimarzo
- 502 [5] P.D. Cani, H. Plovier, M. Van Hul, L. Geurts, N.M. Delzenne, C. Druart, A. Everard. (2016).
503 Endocannabinoids--at the crossroads between the gut microbiota and host metabolism. *Nat Rev Endocrinol*,
504 12(3), 133-143. doi:10.1038/nrendo.2015.211
- 505 [6] V. Di Marzo. (2018). New approaches and challenges to targeting the endocannabinoid system. *Nat Rev*
506 *Drug Discov*, 17(9), 623-639. doi:10.1038/nrd.2018.115
- 507 [7] C.J. Hillard. (2018). Circulating Endocannabinoids: From Whence Do They Come and Where are They
508 Going? *Neuropsychopharmacology*, 43(1), 155-172. doi:10.1038/npp.2017.130
- 509 [8] I.F. Arturo, and Fabiana, P. (2020). Endocannabinoidome. In eLS, John Wiley & Sons, Ltd (Ed.).
510 doi:<https://doi.org/10.1002/9780470015902.a0028301>
- 511 [9] F. Piscitelli, V. Di Marzo. (2012). "Redundancy" of endocannabinoid inactivation: new challenges and
512 opportunities for pain control. *ACS Chem Neurosci*, 3(5), 356-363. doi:10.1021/cn300015x
- 513 [10] V. Di Marzo. (2008). Endocannabinoids: synthesis and degradation. *Rev Physiol Biochem Pharmacol*,
514 160, 1-24. doi:10.1007/112_0505
- 515 [11] S. Castonguay-Paradis, S. Lacroix, G. Rochefort, L. Parent, J. Perron, C. Martin, B. Lamarche, F.
516 Raymond, N. Flamand, V. Di Marzo, A. Veilleux. (2020). Dietary fatty acid intake and gut microbiota
517 determine circulating endocannabinoidome signaling beyond the effect of body fat. *Sci Rep*, 10(1), 15975.
518 doi:10.1038/s41598-020-72861-3

- 519 [12] C. Silvestri, V. Di Marzo. (2013). The endocannabinoid system in energy homeostasis and the
520 etiopathology of metabolic disorders. *Cell Metab*, 17(4), 475-490. doi:10.1016/j.cmet.2013.03.001
- 521 [13] V. Di Marzo, C. Silvestri. (2019). Lifestyle and Metabolic Syndrome: Contribution of the
522 Endocannabinoidome. *Nutrients*, 11(8). doi:10.3390/nu11081956
- 523 [14] N. Forte, A.C. Fernandez-Rilo, L. Palomba, V. Di Marzo, L. Cristino. (2020). Obesity Affects the
524 Microbiota-Gut-Brain Axis and the Regulation Thereof by Endocannabinoids and Related Mediators. *Int J*
525 *Mol Sci*, 21(5). doi:10.3390/ijms21051554
- 526 [15] B. Gatta-Cherifi, D. Cota. (2016). New insights on the role of the endocannabinoid system in the
527 regulation of energy balance. *Int J Obes (Lond)*, 40(2), 210-219. doi:10.1038/ijo.2015.179
- 528 [16] J.D. O'Hare, E. Zielinski, B. Cheng, T. Scherer, C. Buettner. (2011). Central endocannabinoid signaling
529 regulates hepatic glucose production and systemic lipolysis. *Diabetes*, 60(4), 1055-1062. doi:10.2337/db10-
530 0962
- 531 [17] V. Purohit, R. Rapaka, D. Shurtleff. (2010). Role of cannabinoids in the development of fatty liver
532 (steatosis). *AAPS J*, 12(2), 233-237. doi:10.1208/s12248-010-9178-0
- 533 [18] I. Bazwinsky-Wutschke, A. Zipprich, F. Dehghani. (2019). Endocannabinoid System in Hepatic Glucose
534 Metabolism, Fatty Liver Disease, and Cirrhosis. *Int J Mol Sci*, 20(10). doi:10.3390/ijms20102516
- 535 [19] M.A. Karwad, D.G. Couch, E. Theophilidou, S. Sarmad, D.A. Barrett, M. Larvin, K.L. Wright, J.N. Lund,
536 S.E. O'Sullivan. (2017). The role of CB1 in intestinal permeability and inflammation. *FASEB J*, 31(8), 3267-
537 3277. doi:10.1096/fj.201601346R
- 538 [20] K. Kempf, J. Hector, T. Strate, B. Schwarzloh, B. Rose, C. Herder, S. Martin, P. Algenstaedt. (2007).
539 Immune-mediated activation of the endocannabinoid system in visceral adipose tissue in obesity. *Horm Metab*
540 *Res*, 39(8), 596-600. doi:10.1055/s-2007-984459
- 541 [21] M. Maccarrone, I. Bab, T. Biro, G.A. Cabral, S.K. Dey, V. Di Marzo, J.C. Konje, G. Kunos, R.
542 Mechoulam, P. Pacher, K.A. Sharkey, A. Zimmer. (2015). Endocannabinoid signaling at the periphery: 50
543 years after THC. *Trends Pharmacol Sci*, 36(5), 277-296. doi:10.1016/j.tips.2015.02.008
- 544 [22] R. Witkamp. (2016). Fatty acids, endocannabinoids and inflammation. *Eur J Pharmacol*, 785, 96-107.
545 doi:10.1016/j.ejphar.2015.08.051

- 546 [23] A. Nagappan, J. Shin, M.H. Jung. (2019). Role of Cannabinoid Receptor Type 1 in Insulin Resistance and
547 Its Biological Implications. *Int J Mol Sci*, 20(9). doi:10.3390/ijms20092109
- 548 [24] A. Stasiulewicz, K. Znajdek, M. Grudzien, T. Pawinski, A.J.I. Sulkowska. (2020). A Guide to Targeting
549 the Endocannabinoid System in Drug Design. *Int J Mol Sci*, 21(8). doi:10.3390/ijms21082778
- 550 [25] F. Suriano, et al. (2021). Novel insights into the genetically obese (ob/ob) and diabetic (db/db) mice: two
551 sides of the same coin. *Microbiome*, In press.
- 552 [26] E.G. Bligh, W.J. Dyer. (1959). A rapid method of total lipid extraction and purification. *Can J Biochem*
553 *Physiol*, 37(8), 911-917. doi:10.1139/o59-099
- 554 [27] A. Everard, H. Plovier, M. Rastelli, M. Van Hul, A. de Wouters d'Oplinter, L. Geurts, C. Druart, S. Robine,
555 N.M. Delzenne, G.G. Muccioli, W.M. de Vos, S. Luquet, N. Flamand, V. Di Marzo, P.D. Cani. (2019).
556 Intestinal epithelial N-acylphosphatidylethanolamine phospholipase D links dietary fat to metabolic
557 adaptations in obesity and steatosis. *Nat Commun*, 10(1), 457. doi:10.1038/s41467-018-08051-7
- 558 [28] C. Depommier, N. Flamand, R. Pelicaen, D. Maiter, J.-P. Thissen, A. Loumaye, M.P. Hermans, A.
559 Everard, N.M. Delzenne, V. Di Marzo, P.D. Cani. (2021). Linking the Endocannabinoidome with Specific
560 Metabolic Parameters in an Overweight and Insulin-Resistant Population: From Multivariate Exploratory
561 Analysis to Univariate Analysis and Construction of Predictive Models. *Cells*, 10(1), 71.
- 562 [29] F.A. Iannotti, V. Di Marzo. (2020). The gut microbiome, endocannabinoids and metabolic disorders. *J*
563 *Endocrinol*. doi:10.1530/JOE-20-0444
- 564 [30] T.A. Archambault AS, Martin C, Dumais E, Rakotoarivelo V, Laviolette M, Silvestri C, Kostrzewa M,
565 Ligresti A, Boulet LP, Di Marzo V, Flamand N. (2020). Human eosinophils and neutrophils biosynthesize
566 novel 15-lipoxygenase metabolites from 1-linoleoyl-glycerol and N-linoleoyl-ethanolamine. *J Immunol*
567 204(suppl 1): 220.28-220.28.
- 568 [31] G. Gruden, F. Barutta, G. Kunos, P. Pacher. (2016). Role of the endocannabinoid system in diabetes and
569 diabetic complications. *Br J Pharmacol*, 173(7), 1116-1127. doi:10.1111/bph.13226
- 570 [32] D.L. Coleman. (1978). Obese and diabetes: two mutant genes causing diabetes-obesity syndromes in
571 mice. *Diabetologia*, 14(3), 141-148. doi:10.1007/BF00429772
- 572 [33] P.M. Zygmont, A. Ermund, P. Movahed, D.A. Andersson, C. Simonsen, B.A. Jonsson, A. Blomgren, B.
573 Birnir, S. Bevan, A. Eschalier, C. Mallet, A. Gomis, E.D. Hogestatt. (2013). Monoacylglycerols activate

574 TRPV1--a link between phospholipase C and TRPV1. *PLoS One*, 8(12), e81618.
575 doi:10.1371/journal.pone.0081618

576 [34] T.C. Fricke, F. Echtermeyer, J. Zielke, J. de la Roche, M.R. Filipovic, S. Claverol, C. Herzog, M.
577 Tominaga, R.A. Pumroy, V.Y. Moiseenkova-Bell, P.M. Zygmunt, A. Leffler, M.J. Eberhardt. (2019).
578 Oxidation of methionine residues activates the high-threshold heat-sensitive ion channel TRPV2. *Proc Natl*
579 *Acad Sci U S A*, 116(48), 24359-24365. doi:10.1073/pnas.1904332116

580 [35] C.M. Issa, B.D. Hambly, Y. Wang, S. Maleki, W. Wang, J. Fei, S. Bao. (2014). TRPV2 in the development
581 of experimental colitis. *Scand J Immunol*, 80(5), 307-312. doi:10.1111/sji.12206

582 [36] W. Ma, C. Li, S. Yin, J. Liu, C. Gao, Z. Lin, R. Huang, J. Huang, Z. Li. (2015). Novel role of TRPV2 in
583 promoting the cytotoxicity of H₂O₂-mediated oxidative stress in human hepatoma cells. *Free Radic Biol Med*,
584 89, 1003-1013. doi:10.1016/j.freeradbiomed.2015.09.020

585 [37] A. Schiano Moriello, S. Lopez Chinarro, O. Novo Fernandez, J. Eras, P. Amodeo, R. Canela-Garayoa,
586 R.M. Vitale, V. Di Marzo, L. De Petrocellis. (2018). Elongation of the Hydrophobic Chain as a Molecular
587 Switch: Discovery of Capsaicin Derivatives and Endogenous Lipids as Potent Transient Receptor Potential
588 Vanilloid Channel 2 Antagonists. *J Med Chem*, 61(18), 8255-8281. doi:10.1021/acs.jmedchem.8b00734

589 [38] C.E. Ramsden, D. Zamora, A. Makriyannis, J.T. Wood, J.D. Mann, K.R. Faurot, B.A. MacIntosh, S.F.
590 Majchrzak-Hong, J.R. Gross, A.B. Courville, J.M. Davis, J.R. Hibbeln. (2015). Diet-induced changes in n-3-
591 and n-6-derived endocannabinoids and reductions in headache pain and psychological distress. *J Pain*, 16(8),
592 707-716. doi:10.1016/j.jpain.2015.04.007

593 [39] K.C. Verhoeckx, T. Voortman, M.G. Balvers, H.F. Hendriks, M.W. H, R.F. Witkamp. (2011). Presence,
594 formation and putative biological activities of N-acyl serotonin, a novel class of fatty-acid derived mediators,
595 in the intestinal tract. *Biochim Biophys Acta*, 1811(10), 578-586. doi:10.1016/j.bbalip.2011.07.008

596 [40] A. Arshad, W.Y. Chung, W. Steward, M.S. Metcalfe, A.R. Dennison. (2013). Reduction in circulating
597 pro-angiogenic and pro-inflammatory factors is related to improved outcomes in patients with advanced
598 pancreatic cancer treated with gemcitabine and intravenous omega-3 fish oil. *HPB (Oxford)*, 15(6), 428-432.
599 doi:10.1111/hpb.12002

600 [41] J.E. Watson, J.S. Kim, A. Das. (2019). Emerging class of omega-3 fatty acid endocannabinoids & their
601 derivatives. *Prostaglandins Other Lipid Mediat*, 143, 106337. doi:10.1016/j.prostaglandins.2019.106337

602 [42] C.L. Wainwright, L. Michel. (2013). Endocannabinoid system as a potential mechanism for n-3 long-
603 chain polyunsaturated fatty acid mediated cardiovascular protection. *Proc Nutr Soc*, 72(4), 460-469.
604 doi:10.1017/S0029665113003406

605 [43] J. Meijerink, M. Balvers, R. Witkamp. (2013). N-Acyl amines of docosahexaenoic acid and other n-3
606 polyunsaturated fatty acids - from fishy endocannabinoids to potential leads. *Br J Pharmacol*, 169(4), 772-783.
607 doi:10.1111/bph.12030

608 [44] J. Allaire, P. Couture, M. Leclerc, A. Charest, J. Marin, M.C. Lepine, D. Talbot, A. Tchernof, B.
609 Lamarche. (2016). A randomized, crossover, head-to-head comparison of eicosapentaenoic acid and
610 docosahexaenoic acid supplementation to reduce inflammation markers in men and women: the Comparing
611 EPA to DHA (ComparED) Study. *Am J Clin Nutr*, 104(2), 280-287. doi:10.3945/ajcn.116.131896

612 [45] M.G. Balvers, K.C. Verhoeckx, P. Plastina, H.M. Wortelboer, J. Meijerink, R.F. Witkamp. (2010).
613 Docosahexaenoic acid and eicosapentaenoic acid are converted by 3T3-L1 adipocytes to N-acyl ethanolamines
614 with anti-inflammatory properties. *Biochim Biophys Acta*, 1801(10), 1107-1114.
615 doi:10.1016/j.bbaliip.2010.06.006

616 [46] G.G. Muccioli, D. Naslain, F. Backhed, C.S. Reigstad, D.M. Lambert, N.M. Delzenne, P.D. Cani. (2010).
617 The endocannabinoid system links gut microbiota to adipogenesis. *Mol Syst Biol*, 6, 392.
618 doi:10.1038/msb.2010.46

619 [47] M. Bouaboula, S. Hilairret, J. Marchand, L. Fajas, G. Le Fur, P. Casellas. (2005). Anandamide induced
620 PPARgamma transcriptional activation and 3T3-L1 preadipocyte differentiation. *Eur J Pharmacol*, 517(3),
621 174-181. doi:10.1016/j.ejphar.2005.05.032

622 [48] V. Gasperi, F. Fezza, N. Pasquariello, M. Bari, S. Oddi, A.F. Agro, M. Maccarrone. (2007).
623 Endocannabinoids in adipocytes during differentiation and their role in glucose uptake. *Cell Mol Life Sci*,
624 64(2), 219-229. doi:10.1007/s00018-006-6445-4

625 [49] C.E. Rockwell, N.E. Kaminski. (2004). A cyclooxygenase metabolite of anandamide causes inhibition of
626 interleukin-2 secretion in murine splenocytes. *J Pharmacol Exp Ther*, 311(2), 683-690.
627 doi:10.1124/jpet.104.065524

628 [50] S.E. O'Sullivan. (2016). An update on PPAR activation by cannabinoids. *Br J Pharmacol*, 173(12), 1899-
629 1910. doi:10.1111/bph.13497

630 [51] M. Alhouayek, G.G. Muccioli. (2014). Harnessing the anti-inflammatory potential of
631 palmitoylethanolamide. *Drug Discov Today*, 19(10), 1632-1639. doi:10.1016/j.drudis.2014.06.007

632 [52] S. Petrosino, V. Di Marzo. (2017). The pharmacology of palmitoylethanolamide and first data on the
633 therapeutic efficacy of some of its new formulations. *Br J Pharmacol*, 174(11), 1349-1365.
634 doi:10.1111/bph.13580

635 [53] M. Ohara, S. Ohnishi, H. Hosono, K. Yamamoto, Q. Fu, O. Maehara, G. Suda, N. Sakamoto. (2018).
636 Palmitoylethanolamide Ameliorates Carbon Tetrachloride-Induced Liver Fibrosis in Rats. *Front Pharmacol*,
637 9, 709. doi:10.3389/fphar.2018.00709

638 [54] J. Paloczi, Z.V. Varga, G. Hasko, P. Pacher. (2018). Neuroprotection in Oxidative Stress-Related
639 Neurodegenerative Diseases: Role of Endocannabinoid System Modulation. *Antioxid Redox Signal*, 29(1),
640 75-108. doi:10.1089/ars.2017.7144

641 [55] C. Turcotte, M.R. Blanchet, M. Laviolette, N. Flamand. (2016). The CB2 receptor and its role as a
642 regulator of inflammation. *Cell Mol Life Sci*, 73(23), 4449-4470. doi:10.1007/s00018-016-2300-4

643 [56] G.G. Muccioli. (2010). Endocannabinoid biosynthesis and inactivation, from simple to complex. *Drug*
644 *Discov Today*, 15(11-12), 474-483. doi:10.1016/j.drudis.2010.03.007

645 [57] C. Lefort, M. Roumain, M. Van Hul, M. Rastelli, R. Manco, I. Leclercq, N.M. Delzenne, V.D. Marzo, N.
646 Flamand, S. Luquet, C. Silvestri, G.G. Muccioli, P.D. Cani. (2020). Hepatic NAPE-PLD Is a Key Regulator
647 of Liver Lipid Metabolism. *Cells*, 9(5), 1247.

648 [58] E. Margheritis, B. Castellani, P. Magotti, S. Peruzzi, E. Romeo, F. Natali, S. Mostarda, A. Gioiello, D.
649 Piomelli, G. Garau. (2016). Bile Acid Recognition by NAPE-PLD. *ACS Chem Biol*, 11(10), 2908-2914.
650 doi:10.1021/acscchembio.6b00624

651 [59] E. Ricciotti, G.A. FitzGerald. (2011). Prostaglandins and inflammation. *Arterioscler Thromb Vasc Biol*,
652 31(5), 986-1000. doi:10.1161/ATVBAHA.110.207449

653 [60] C. Wang, W. Liu, L. Yao, X. Zhang, X. Zhang, C. Ye, H. Jiang, J. He, Y. Zhu, D. Ai. (2017).
654 Hydroxyeicosapentaenoic acids and epoxyeicosatetraenoic acids attenuate early occurrence of nonalcoholic
655 fatty liver disease. *Br J Pharmacol*, 174(14), 2358-2372. doi:10.1111/bph.13844

656 [61] N.D. Hung, M.R. Kim, D.E. Sok. (2011). Mechanisms for anti-inflammatory effects of 1-[15(S)-
657 hydroxyeicosapentaenoyl] lysophosphatidylcholine, administered intraperitoneally, in zymosan A-induced
658 peritonitis. *Br J Pharmacol*, 162(5), 1119-1135. doi:10.1111/j.1476-5381.2010.01117.x

659 [62] P.D. Cani, J. Amar, M.A. Iglesias, M. Poggi, C. Knauf, D. Bastelica, A.M. Neyrinck, F. Fava, K.M.
660 Tuohy, C. Chabo, A. Waget, E. Delmee, B. Cousin, T. Sulpice, B. Chamontin, J. Ferrieres, J.F. Tanti, G.R.
661 Gibson, L. Casteilla, N.M. Delzenne, M.C. Alessi, R. Burcelin. (2007). Metabolic endotoxemia initiates
662 obesity and insulin resistance. *Diabetes*, 56(7), 1761-1772. doi:10.2337/db06-1491

663 [63] P.D. Cani, R. Bibiloni, C. Knauf, A. Waget, A.M. Neyrinck, N.M. Delzenne, R. Burcelin. (2008). Changes
664 in gut microbiota control metabolic endotoxemia-induced inflammation in high-fat diet-induced obesity and
665 diabetes in mice. *Diabetes*, 57(6), 1470-1481. doi:10.2337/db07-1403

666 [64] P. Brun, I. Castagliuolo, V. Di Leo, A. Buda, M. Pinzani, G. Palu, D. Martines. (2007). Increased intestinal
667 permeability in obese mice: new evidence in the pathogenesis of nonalcoholic steatohepatitis. *Am J Physiol*
668 *Gastrointest Liver Physiol*, 292(2), G518-525. doi:10.1152/ajpgi.00024.2006

669 [65] M. Zhao, X. Chen. (2015). Effect of lipopolysaccharides on adipogenic potential and premature
670 senescence of adipocyte progenitors. *Am J Physiol Endocrinol Metab*, 309(4), E334-344.
671 doi:10.1152/ajpendo.00601.2014

672 [66] Q. Zeng, D. Li, Y. He, Y. Li, Z. Yang, X. Zhao, Y. Liu, Y. Wang, J. Sun, X. Feng, F. Wang, J. Chen, Y.
673 Zheng, Y. Yang, X. Sun, X. Xu, D. Wang, T. Kenney, Y. Jiang, H. Gu, Y. Li, K. Zhou, S. Li, W. Dai. (2019).
674 Discrepant gut microbiota markers for the classification of obesity-related metabolic abnormalities. *Sci Rep*,
675 9(1), 13424. doi:10.1038/s41598-019-49462-w

676 [67] O. Rom, Y. Liu, Z. Liu, Y. Zhao, J. Wu, A. Ghayeb, L. Villacorta, Y. Fan, L. Chang, L. Wang, C. Liu,
677 D. Yang, J. Song, J.C. Rech, Y. Guo, H. Wang, G. Zhao, W. Liang, Y. Koike, H. Lu, T. Koike, T. Hayek, S.
678 Pennathur, C. Xi, B. Wen, D. Sun, M.T. Garcia-Barrio, M. Aviram, E. Gottlieb, I. Mor, W. Liu, J. Zhang, Y.E.
679 Chen. (2020). Glycine-based treatment ameliorates NAFLD by modulating fatty acid oxidation, glutathione
680 synthesis, and the gut microbiome. *Sci Transl Med*, 12(572). doi:10.1126/scitranslmed.aaz2841

681

682

683 **Figure legends**

684 **Figure 1:** Different hepatic eCBome tone in *ob/ob* and *db/db* mice. (a) Concentrations of the eCBome-related
685 mediators in the liver tissue (fmol/mg wet tissue weight) measured by HPLC-MS/MS. (b) mRNA expression
686 of receptors and metabolic enzymes for 2-monoacylglycerols and *N*-acylethanolamines measured by qPCR-
687 based TaqMan Open Array. Green: CT *ob* lean mice, red: *ob/ob* mice, blue CT *db* lean mice, and
688 violet: *db/db* mice. Data are presented as the mean \pm S.E.M of n=8-10. * $P \leq 0.05$, ** $P \leq 0.01$, *** $P \leq 0.005$,
689 **** $P \leq 0.001$. For mRNA expression, relative units were calculated versus the mean of the CT *ob* mice values
690 set at 1. Data were analyzed by one-way ANOVA followed by Tukey's post hoc test. Abbreviations: see
691 supplemental Table S1 and Table S2.

692 **Figure 2:** Different eCBome tone in the subcutaneous adipose tissue of *ob/ob* and *db/db* mice. (a)
693 Concentrations of the eCBome-related mediators in the subcutaneous adipose tissue (fmol/mg wet tissue
694 weight) measured by HPLC-MS/MS. (b) mRNA expression of receptors and metabolic enzymes for 2-
695 monoacylglycerols and *N*-acylethanolamines measured by qPCR-based TaqMan Open Array. Green: CT *ob*
696 lean mice, red: *ob/ob* mice, blue CT *db* lean mice, and violet: *db/db* mice. Data are presented as the mean \pm
697 S.E.M of n=8-10. * $P \leq 0.05$, ** $P \leq 0.01$, **** $P \leq 0.001$. For mRNA expression, relative units were calculated
698 versus the mean of the CT *ob* mice values set at 1. Data were analyzed by one-way ANOVA followed by
699 Tukey's post hoc test. Abbreviations: see supplemental Table S1 and Table S2.

700 **Figure 3:** Different eCBome tone in the visceral adipose tissue of *ob/ob* and *db/db* mice. (a) Concentration of
701 the eCBome-related mediators in the visceral adipose tissue (fmol/mg wet tissue weight) measured by HPLC-
702 MS/MS. (b) mRNA expression of receptors and metabolic enzymes for 2-monoacylglycerols and *N*-
703 acylethanolamines measured by qPCR-based TaqMan Open Array. Green: CT *ob* lean mice, red: *ob/ob* mice,
704 blue CT *db* lean mice, and violet: *db/db* mice. Data are presented as the mean \pm S.E.M of n=8-10. ** $P \leq 0.01$,
705 *** $P \leq 0.005$, **** $P \leq 0.001$. For mRNA expression, relative units were calculated versus the mean of the CT
706 *ob* mice values set at 1. Data were analyzed by one-way ANOVA followed by Tukey's post hoc test.
707 Abbreviations: see supplemental Table S1 and Table S2.

708 **Figure 4:** Correlation plot between altered metabolic parameters and eCBome-related mediators and mRNAs
709 measured in the liver. Correlation matrix showing Pearson correlations with Bonferroni's adjustment in the

710 liver. Positive correlations are shown in blue and negative correlations in red. Color intensity and size of the
711 circles are proportional to the correlation coefficients. "X" refers to the first data set, the metabolic parameters
712 measured in the liver while "Y" refers to the second data set, eCBome-related mediators and mRNAs measured
713 in the liver.

714 **Figure 5:** Correlation plot between altered metabolic parameters and the eCBome-related mediators and
715 mRNAs measured in the two adipose tissue depots. (a) Correlation matrix showing Pearson correlations with
716 Bonferroni's adjustment in the subcutaneous adipose tissue; (b) Correlation matrix showing Pearson
717 correlations with Bonferroni's adjustment in the visceral adipose tissue. Positive correlations are displayed in
718 blue and negative correlations in red. Color intensity and size of the circles are proportional to the correlation
719 coefficients. "X" refers to the first data set, the metabolic parameters measured in the two respective adipose
720 tissue depots while "Y" refers to the second data set, the eCBome-related mediators and mRNAs measured in
721 the two respective adipose tissue depots.

722 **Figure 6:** Correlation plot between altered bacterial taxa and eCBome-related mediators and mRNAs
723 measured in the liver tissue. Correlation matrix (Pearson with Bonferroni's adjustment); positive correlations
724 are displayed in blue and negative correlations in red. Color intensity and size of the circles are proportional
725 to the correlation coefficients. "X" refers to the first data set, the altered bacterial taxa while "Y" refers to the
726 second data set, the eCBome-related mediators and mRNAs measured in the liver.

727 **Figure 7:** Correlation plot between altered bacterial taxa and the eCBome-related mediators and mRNAs
728 measured in the two adipose tissue depots. (a) Subcutaneous adipose tissue; (b) Visceral adipose tissue.
729 Correlation matrix (Pearson with Bonferroni's adjustment); positive correlations are displayed in blue and
730 negative correlations in red. Color intensity and size of the circles are proportional to the correlation
731 coefficients. "X" refers to the first data set, the altered bacterial taxa while "Y" refers to the second data set,
732 the eCBome-related mediators and mRNAs measured in the two respective adipose tissue depots.

733

734 **Legends to the supplemental information files**

735 **Supplemental Table S1:** Abbreviations of endocannabinoids and endocannabinoid-like molecules measured
736 in three different tissues (i.e., liver, subcutaneous and visceral adipose tissues).

737 **Supplemental Table S2:** List of the genes analyzed by qPCR based TaqMan Open Array in three different
738 tissues (i.e., liver, subcutaneous and visceral adipose tissues), and their metabolic function.

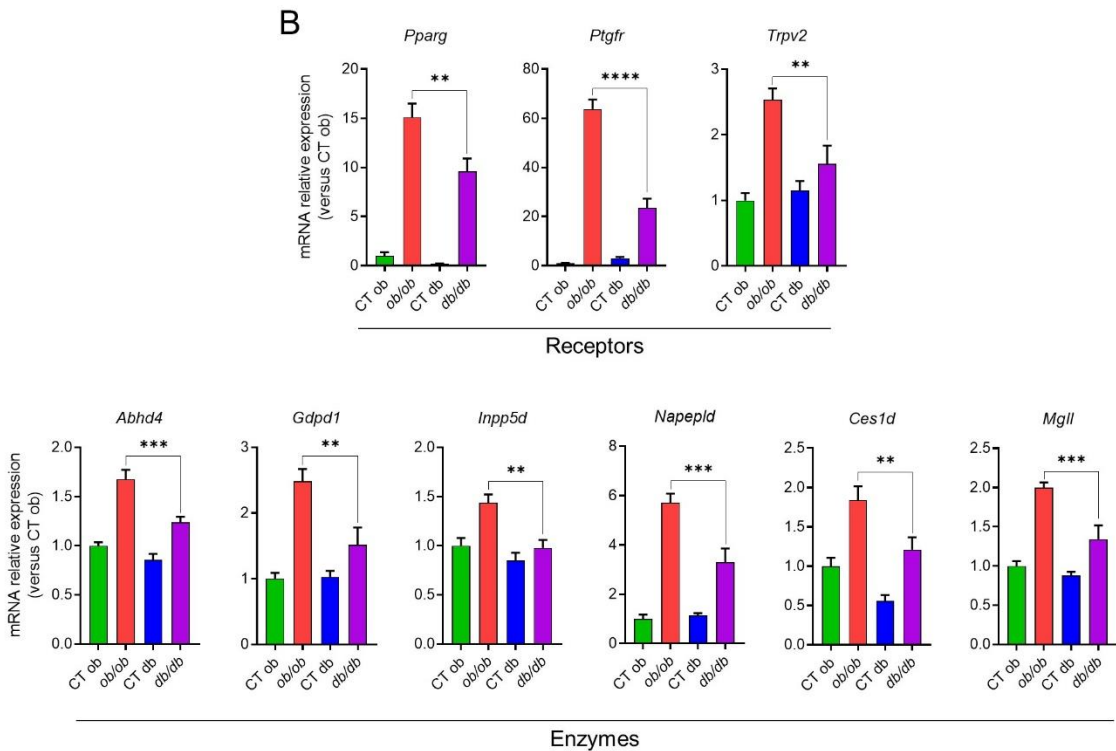
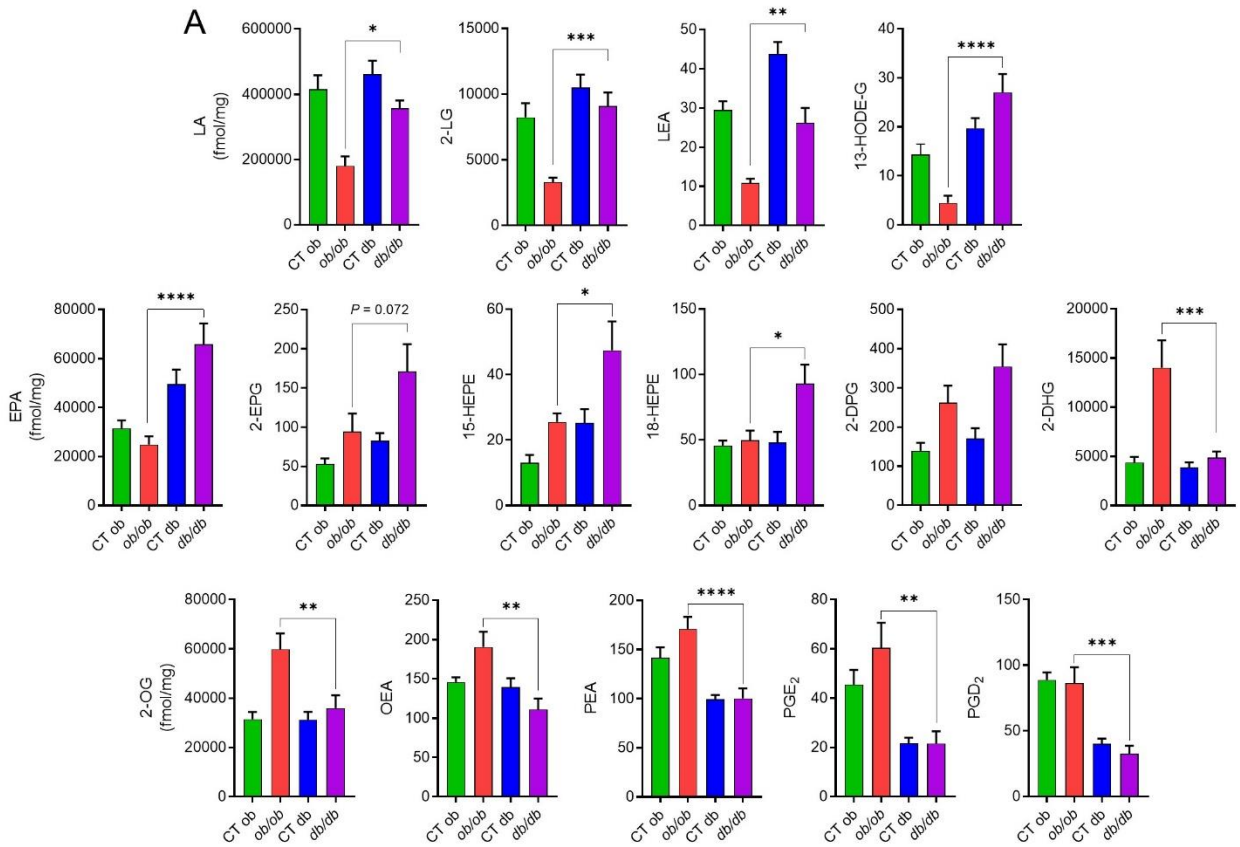
739 **Supplemental Table S3:** mRNA relative expression levels of receptors and metabolic enzymes for 2-
740 monoacylglycerols and *N*-acylethanolamines measured by qPCR-based TaqMan Open Array in the liver tissue
741 of *ob/ob* and *db/db* mice, and their respective littermates. Data are presented as the mean \pm S.E.M of n=8-10.
742 * $P \leq 0.05$, ** $P \leq 0.01$, *** $P \leq 0.005$, **** $P \leq 0.001$. Values are expressed as relative units calculated versus
743 the mean of the CT ob mice values set at 1, and analyzed by one-way ANOVA. Abbreviations: see
744 supplemental Table S1 and Table S2.

745 **Supplemental Table S4:** mRNA relative expression levels of receptors and metabolic enzymes for 2-
746 monoacylglycerols and *N*-acylethanolamines measured by qPCR-based TaqMan Open Array in the
747 subcutaneous adipose tissue of *ob/ob* and *db/db* mice, and their respective littermates. Data are presented as
748 the mean \pm S.E.M of n=8-10. Values are expressed as relative units calculated versus the mean of the CT ob
749 mice values set at 1, and analyzed by one-way ANOVA. Abbreviations: see supplemental Table S1 and Table
750 S2.

751 **Supplemental Table S5:** mRNA relative expression levels of receptors and metabolic enzymes for 2-
752 monoacylglycerols and *N*-acylethanolamines measured by qPCR-based TaqMan Open Array in the visceral
753 adipose tissue of *ob/ob* and *db/db* mice, and their respective littermates. Data are presented as the mean \pm
754 S.E.M of n=8-10. * $P \leq 0.05$, *** $P \leq 0.005$. Values are expressed as relative units calculated versus the mean
755 of the CT ob mice values set at 1, and analyzed by one-way ANOVA. Abbreviations: see supplemental Table
756 S1 and Table S2.

757 **Supplemental Table S6:** List of the deuterated internal standards used for LC/MS-MS analyses

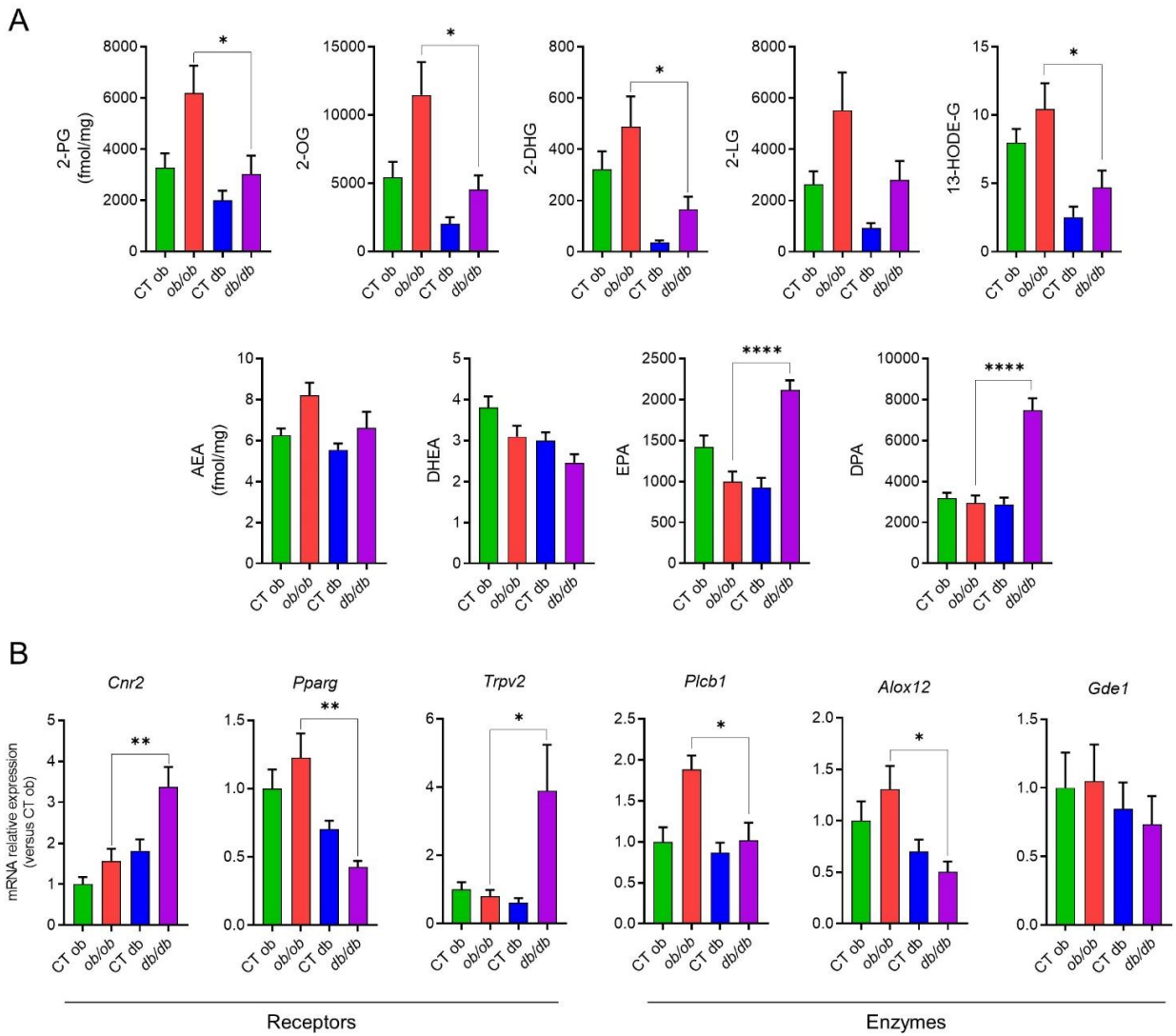
758



759

760 Fig. 1

761



762

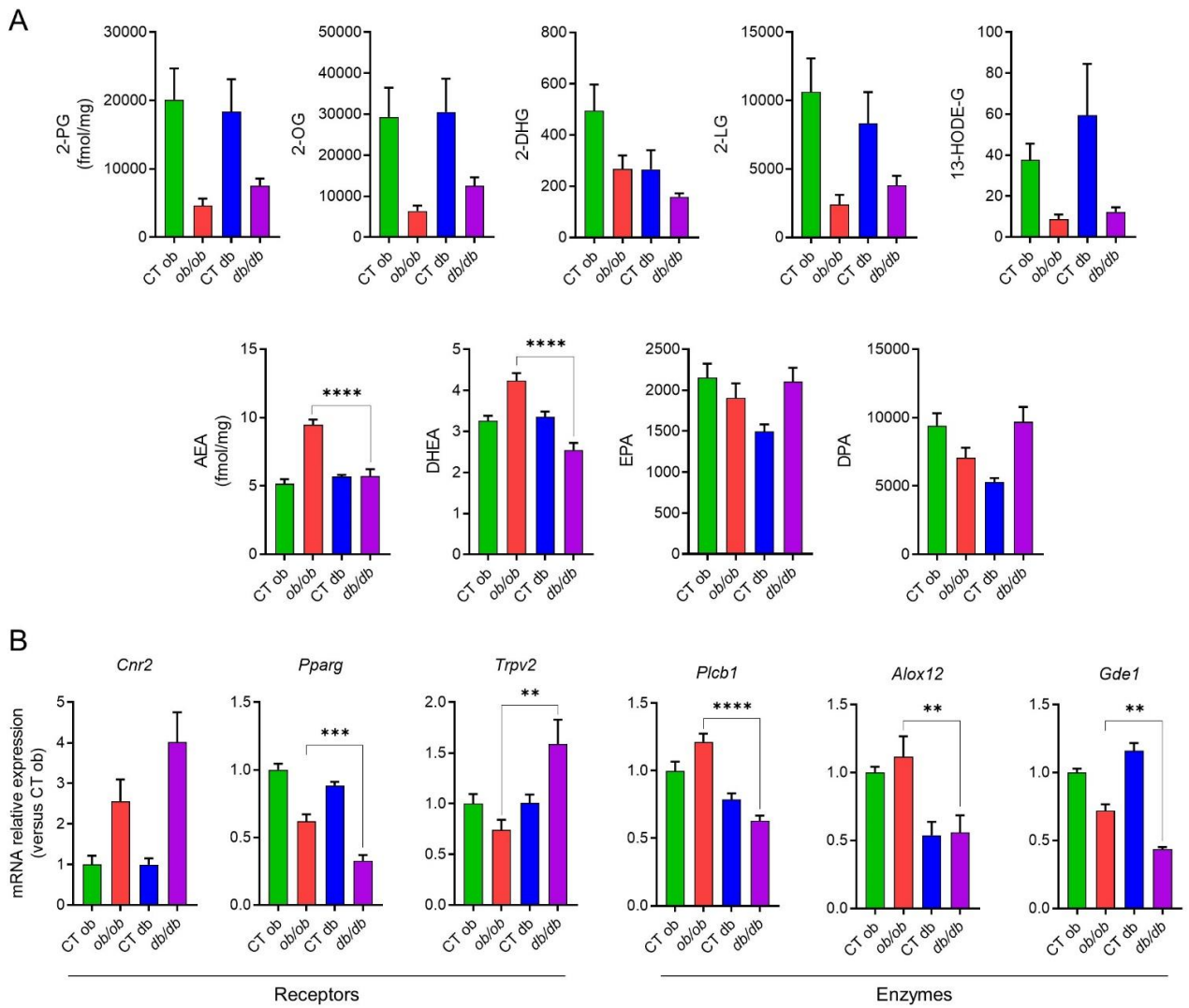
763 Fig. 2

764

765

766

767



768

769 Fig. 3

770

771

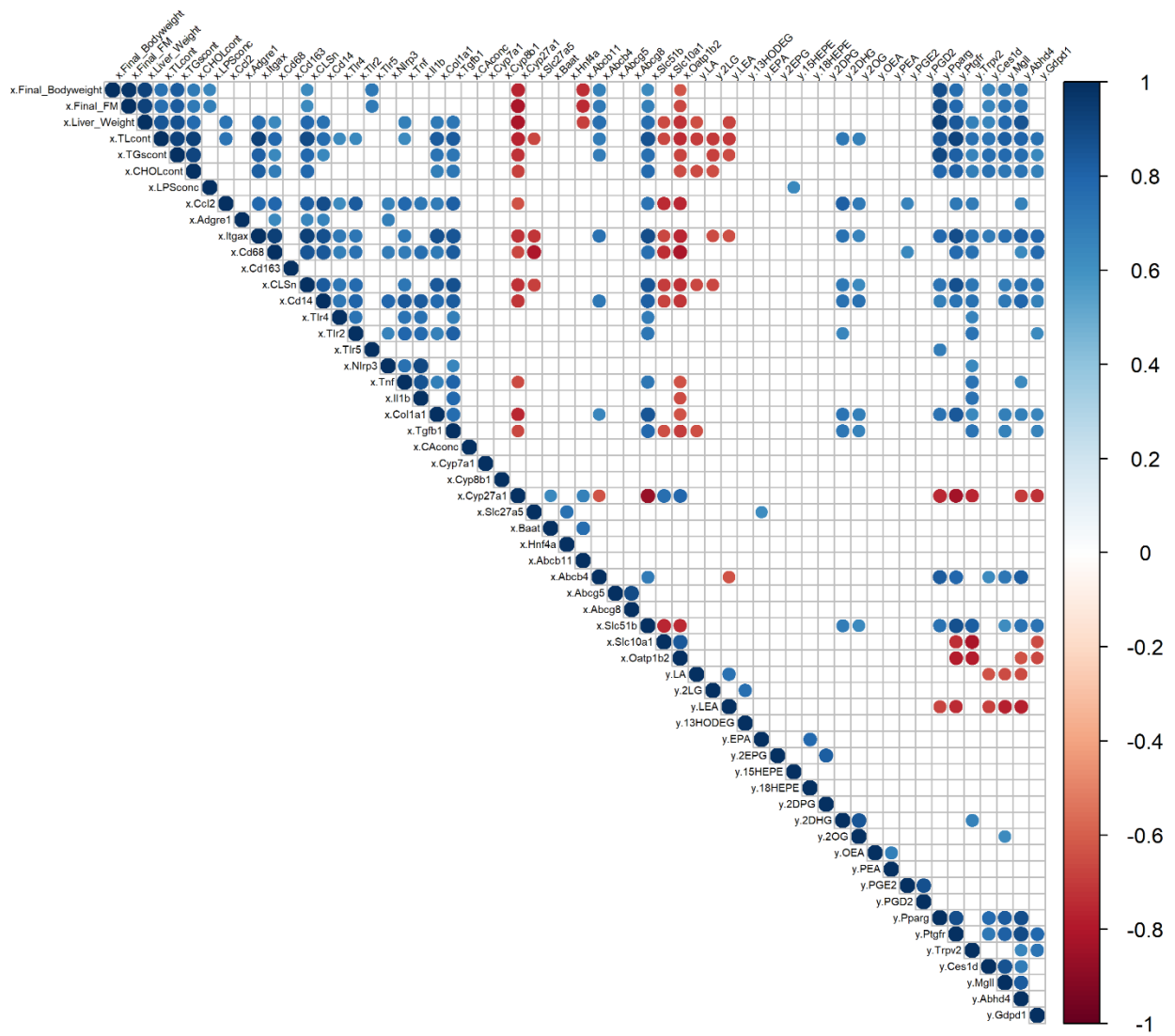
772

773

774

775

776



777

778 Fig. 4

779

780

781

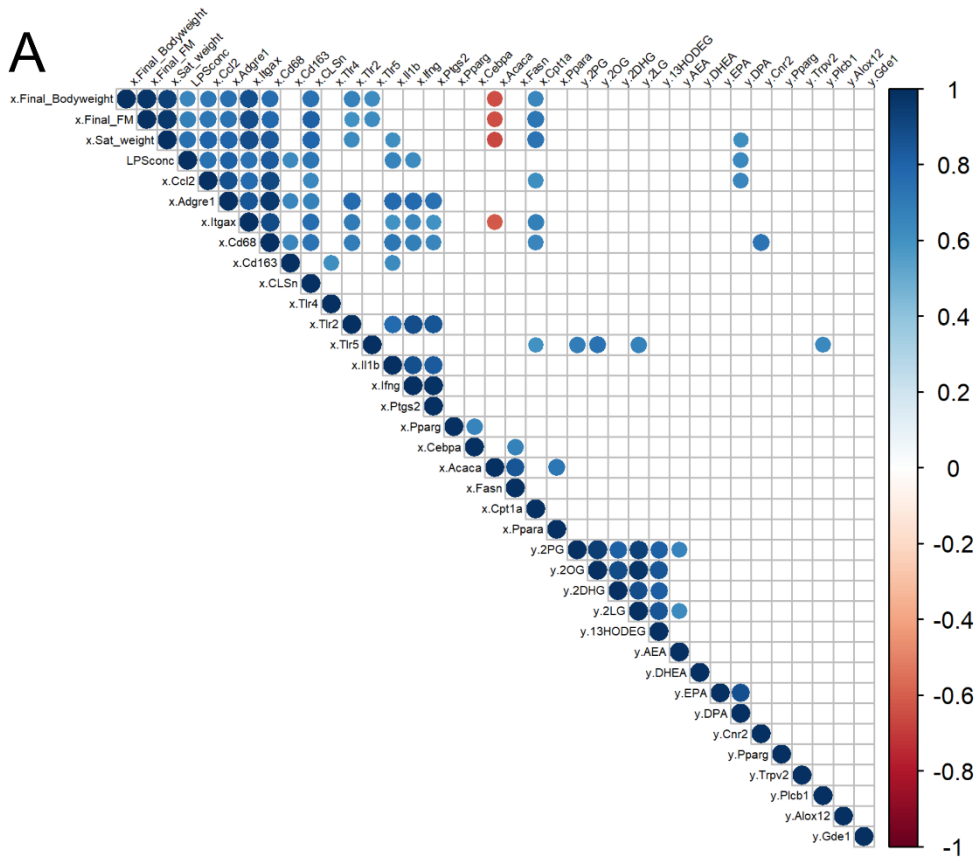
782

783

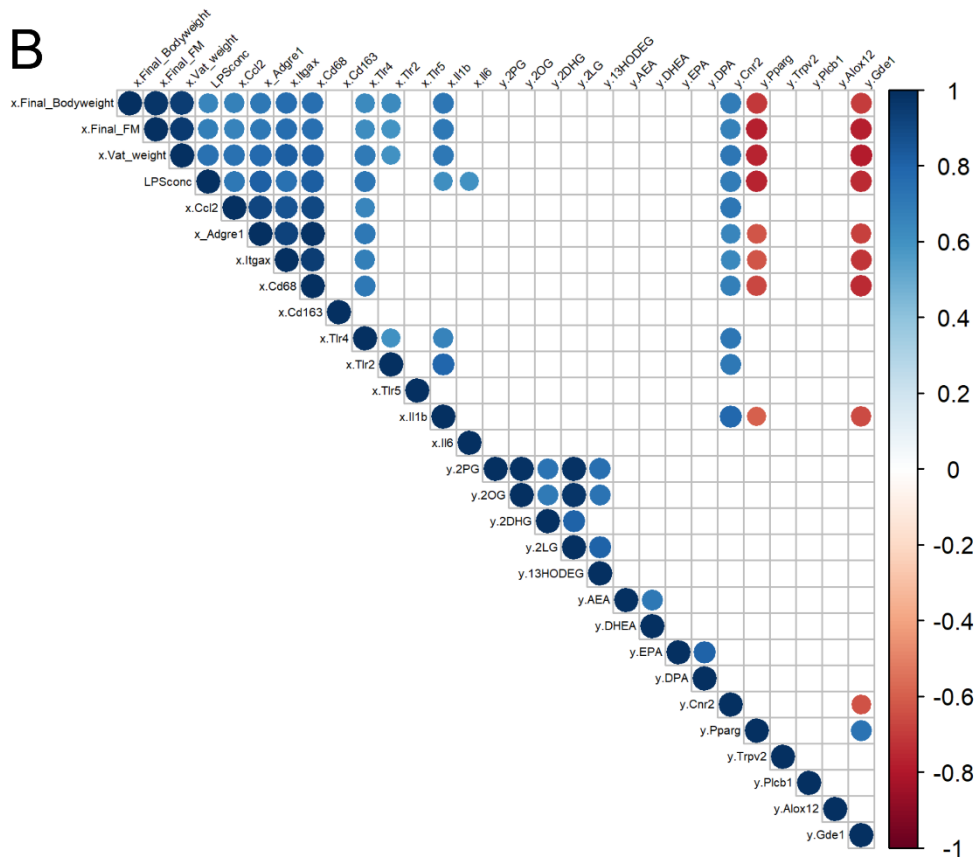
784

785

A

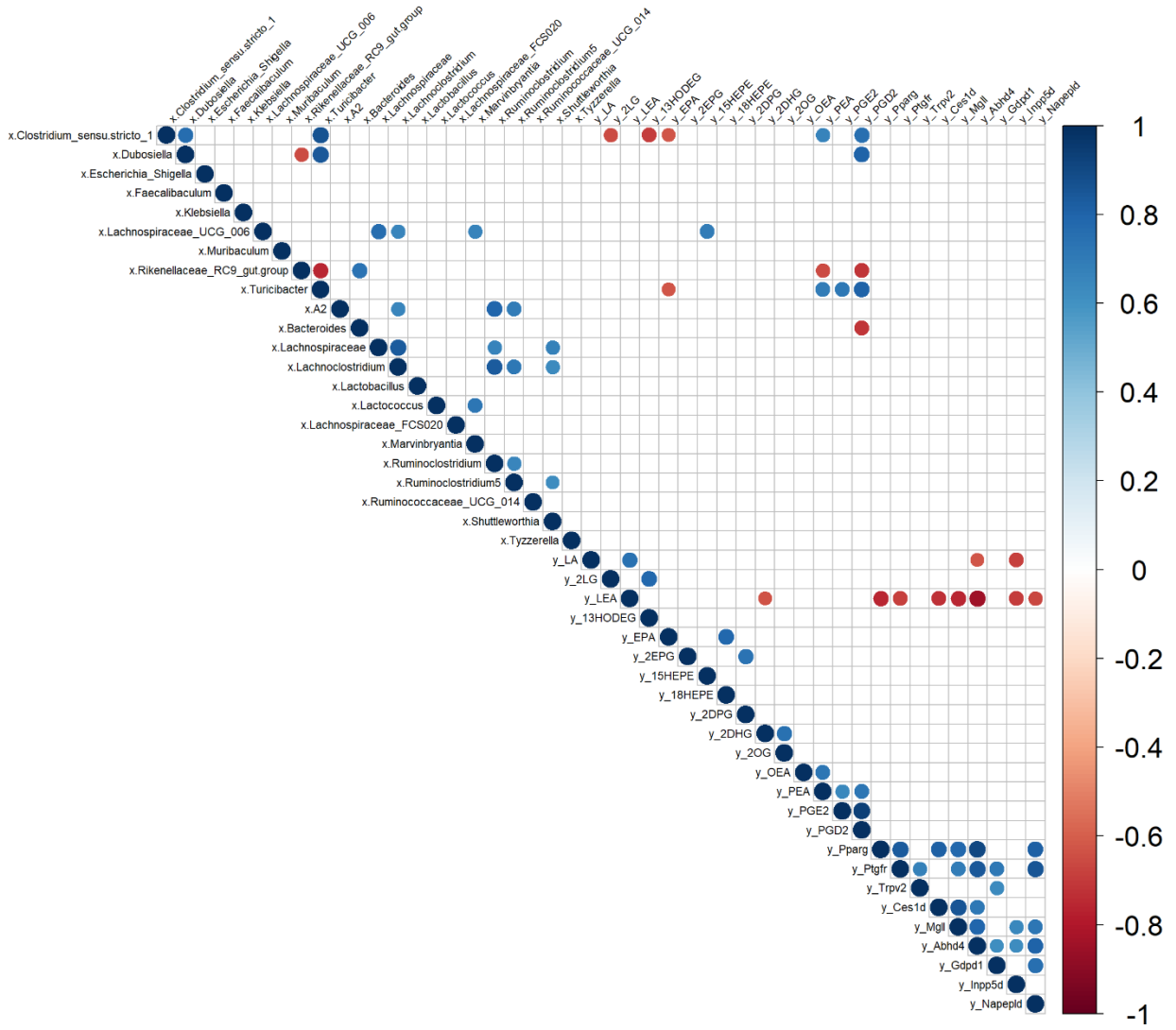


B



786

787 Fig. 5



788

789 Fig. 6

790

791

792

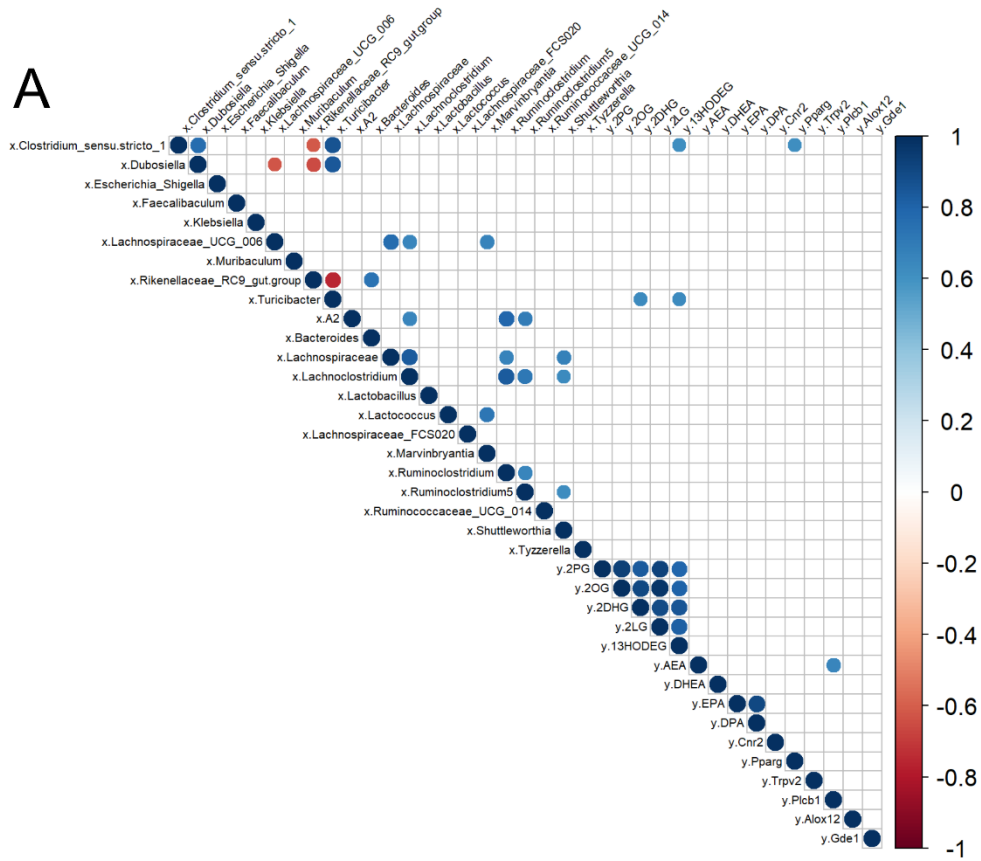
793

794

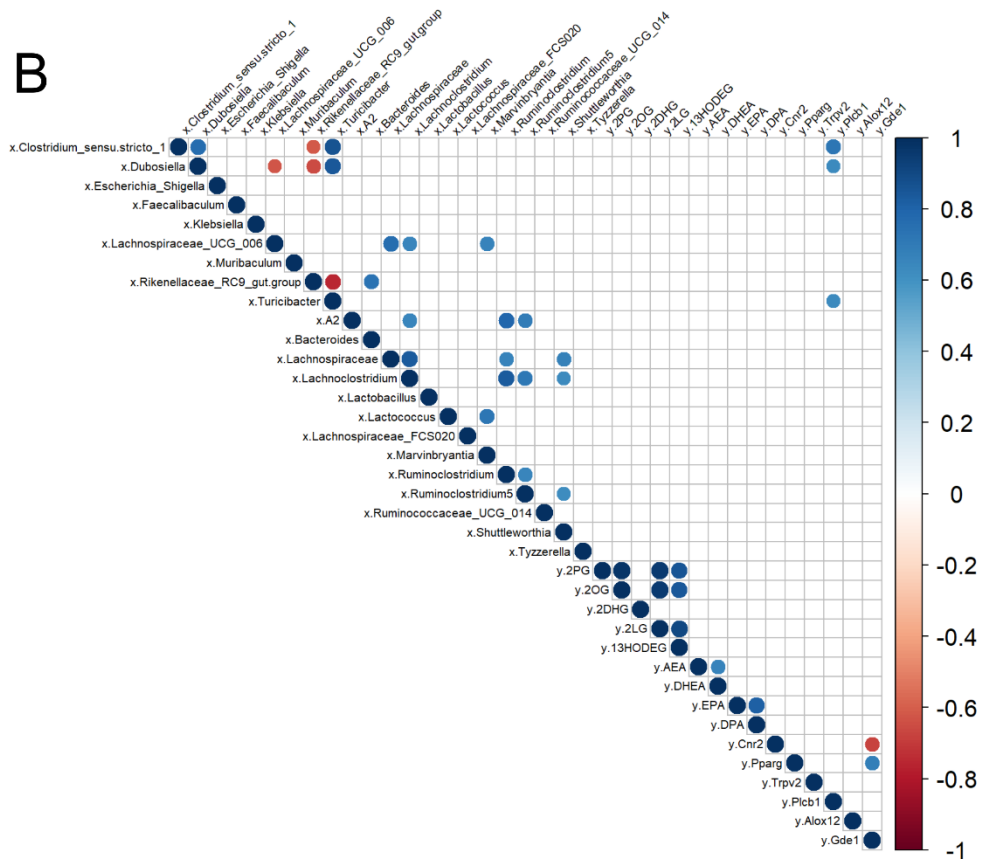
795

796

A



B



797

798 Fig. 7